A novel repressor of the *ica* locus discovered from clinically isolated super biofilm-elaborating *Staphylococcus aureus*

Liansheng Yu [a], Junzo Hisatsune [a,b], Ikue Hayashi [c], Nobuyuki Tatsukawa [a], Yusuke Sato'o [a], Emiri Mizumachi [a], Fuminori Kato [a,b], Hideki Hirakawa[d], Gerald B. Pier [e], Motoyuki Sugai [a,b]

[a]Department of Bacteriology, Hiroshima University Graduate School of Biomedical & Health Sciences, Hiroshima City, Hiroshima, Japan; [b]Project Research Center for Nosocomial Infectious Diseases, Hiroshima University, Hiroshima, Japan; [c]Research Facility, Hiroshima University Faculty of Dentistry, Hiroshima City, Hiroshima, Japan; [d]Genome Informatics Group, Department of Technology Development, Kazusa DNA Research Institute; [e]Division of Infectious Diseases, Department of Medicine, Brigham and Women's Hospital, and Harvard Medical School, Boston, MA 02115

Running Head: Biofilm regulation by *rob* in *S. aureus*

Address correspondence to Motoyuki Sugai, sugai@hiroshima-u.ac.jp

ABSTRACT

Staphylococcus aureus TF2758 is a clinical isolate from an atheroma and a super biofilm-elaborating/PIA/PNAG-overproducing strain (S. Looniva et al. Microbiol. Immunol. 60, 148-159, 2016). A microarray analysis and DNA genome sequencing were performed to identify the mechanism underlying biofilm overproduction by TF2758. We found high transcriptional expression levels of a 7-gene cluster (*satf2580* - *satf2586*) and the *ica* operon in TF2758. Within the 7-gene cluster, a putative transcriptional regulator gene designated as *rob* had a nonsense mutation that caused the truncation of the protein. The complementation of TF2758 with *rob* from FK300, an *rsbU*-repaired *S. aureus* strain NCTC8325-4, significantly decreased biofilm elaboration, suggesting a role for *rob* in this process. The deletion of *rob* in biofilm-non-producing FK300 significantly increased biofilm elaboration and PIA/PNAG production. In the search for gene(s) in the 7-gene cluster for biofilm elaboration controlled by *rob*, we identified *orf* SAOUHSC_2898 (*satf2584*). Our results suggest that *orf* SAOUHSC_2898 (*satf2584*) and *icaADBC* are required for enhanced biofilm elaboration and PIA/PNAG production in the *rob* deletion mutant. Rob bound to a palindromic sequence within its own promoter region. Furthermore, Rob recognized the TATTT motif within the *icaR-icaA* intergenic region and bound to a 25-bp DNA stretch containing this motif, which is a critically important short sequence regulating biofilm elaboration in *S. aureus*. Our results strongly suggest that Rob is a long-sought repressor that recognizes and binds to the TATTT motif and is an important regula-

39 tor of biofilm elaboration through its control of SAOUHSC_2898 (SATF2584) and Ica protein

40 expression in *S. aureus*.

41

42 **IMPORTANCE**

43 During the search for molecular mechanism underlying biofilm overproduction of *Staphylococ-*

44 *cus aureus* TF2758, we found a putative transcriptional regulator gene designated as *rob* within a

45 7-gene cluster showing high transcriptional expression level by microarray analysis. The deletion

46 of *rob* in biofilm-non-producing FK300, an *rsbU*-repaired NCTC8325-4, significantly increased

47 biofilm elaboration and PIA/PNAG production. Search for gene(s) in the 7-gene cluster for bio-

48 film elaboration controlled by *rob* identified *orf* SAOUHSC_2898. Besides binding to its own

49 promoter region to control *orf* SAOUHSC_2898 expression, Rob recognized the TATTT motif

50 within the *icaR-icaA* intergenic region and bound to a 25-bp DNA stretch containing this motif,

51 which is a critically important short sequence regulating biofilm elaboration in *S. aureus*. Our

52 results strongly suggest that Rob is a long-sought repressor that recognizes and binds to the

53 TATTT motif and is a new important regulator of biofilm elaboration through its control of

54 SAOUHSC_2898 and Ica protein expression in *S. aureus*.

55

56

57 *Staphylococcus aureus* is among the most common human pathogens, causing a wide range
58 of infections, from superficial skin and mucosal infections to bone or lung infections, as well as
59 serious systemic diseases. *S. aureus* colonization has been regarded as a risk factor for develop-
60 ing subsequent infections. Some chronic infections, such as endocarditis, osteomyelitis, and
61 those on implanted medical devices, are characteristically associated with biofilm elaboration
62 (1-3). Development of biofilms has been divided into at least three physiologically different
63 stages: initial attachment, biofilm maturation, and detachment (or dispersal), which involves
64 specific factors (4). The matrix of a staphylococcal biofilm is mainly composed of polysaccha-
65 rides, cell surface and secreted bacterial proteins, and extracellular DNA (5). Cells encased in the
66 matrix are protected from antibiotic therapy and host immune responses (3, 4, 6). Dispersal of
67 cells from a biofilm may be important for the dissemination of the bacteria (7).
68 The main exopolysaccharide of the *S. aureus* biofilm matrix is poly-*N*-acetylglucosamine
69 (PNAG), which is also known as polysaccharide intercellular adhesion (PIA) (8). The synthesis
70 and accumulation of PIA/PNAG on the cell surface is carried out by the products of four genes:
71 *icaA*, *icaD*, *icaB*, and *icaC* (9). These genes are located in one operon and were first identified by
72 Heilmann et al. (10). Recent studies have indicated that the expression of *icaADBC* is affected by
73 a number of regulatory and environmental factors (11-14). The *icaR* gene is located adjacent to
74 *icaADBC*, but is divergently transcribed from this operon (15). The protein encoded by *icaR* be-
75 longs to the TetR family of transcriptional regulators and represses *icaADBC* transcription by

76 binding to a region immediately upstream of the *icaA* start codon (16). Additionally, environ-
77 mental factors, including glucose, ethanol, high temperatures, and high osmolarity, have been
78 reported to affect biofilm elaboration (11-14). Ethanol increases the expression of *icaA* by re-
79 pressing *icaR* transcription (15). In contrast, enhancement of *icaA* expression by high glucose or
80 NaCl levels was found to occur independently of *icaR*.

81 A 5-nucleotide motif (TATTT) within the *icaR-icaA* intergenic region was previously shown
82 to play a key role in the transcription of the *ica* locus (16). This study also demonstrated that Ic-
83 aR binds to a 42-bp sequence within the *ica* promoter region, but not the TATTT sequence.
84 Hence, the effects of the TATTT motif on *icaADBC* expression have been suggested to be con-
85 trolled by other as yet unidentified repressor(s).

86 We evaluated the biofilm-elaborating ability of clinical isolates in Japan, and found that
87 TF2758, which was isolated from an atheroma, is an extremely high biofilm producer (17).
88 Whole-genome sequencing and a microarray analysis of TF2758 discovered a spontaneous mu-
89 tation in a putative transcriptional regulator gene, within a 7-gene cluster, which was expressed
90 at markedly higher levels than in a non-biofilm elaborating control strain. We designated this
91 gene as *rob*, regulator of biofilm. In the present study, we demonstrate that Rob is a long-sought
92 repressor that recognizes and binds to the TATTT motif and suggest that Rob is an important
93 regulator of biofilm elaboration through its control of the expression of an as yet uncharacterized
94 hypothetical protein SAOUHSC_2898 (SATF2584) and IcaADBC.

95

96 **RESULTS**

97 **Identification of *rob* from a super biofilm-elaborating strain.** As shown in Fig. 1, one of the
98 clinically isolated strains, TF2758, showed a strong biofilm-elaborating ability and hyperproduc-
99 tion of PIA/PNAG (17). In order to elucidate the mechanism underlying the overproduction of
100 biofilms in TF2758, a gene expression analysis using a custom microarray was performed. We
101 used ATCC49775 as a control because it was the strain most closely related to TF2758 by com-
102 parative genomic hybridization and a very low biofilm-elaborating strain (Fig. 1A, B). The re-
103 sults obtained showed that there were two strongly up-regulated gene clusters: *satf2580* –
104 *satf2586* (15-to-40-fold) and the *ica* operon (*satf2686* – *satf2689*, 2-to-10-fold) (Fig. 1C, Table
105 S1). Sequencing of the TF2758 genome and comparisons with complete genomes of other *S. au-*
106 *reus* strains indicated that TF2758 possessed a nonsense mutation in the gene *satf2583* (Fig. 2A)
107 and a missense mutation in the gene *icaR*, which resulted in the creation of a stop codon and an
108 alteration in a nucleotide (A to T), respectively (Fig. S1 in the supplemental material). SATF2583
109 possessed regions homologous to the TetR family and AcrR family of transcriptional regulators,
110 suggesting it acts as a DNA-binding protein (Fig. 2B). In order to clarify the impact of
111 SATF2583 on biofilm elaboration in *S. aureus*, we transformed TF2758 with the plasmid pC001,
112 pKAT carrying *orf*SAOUHSC_2897 with a 5'-flanking region cloned from FK300, the *rsbU* re-
113 paired derivative of NCTC8325-4. As shown in Figure 3A, TF2758 carrying pC001 significantly

114 lost its biofilm-elaborating ability, particularly in the absence of 1% glucose. PIA/PNAG detec-
115 tion by anti-PNAG revealed more clear-cut data (Fig. 3B). In the presence of 1% glucose,
116 TF2758 carrying pC001 still retained its PIA/PNAG-producing ability; however, the amount
117 produced was markedly less than that by the wild type. However, the production of PIA/PNAG
118 was almost completely inhibited in the absence of 1% glucose. These results suggest that
119 SATF2583 is a negative regulator of biofilm elaboration and also that the *satf2583* gene from
120 FK300 is functional.

121 The *icaR* gene, located adjacent to the *ica* operon, is a member of the TetR family of tran-
122 scriptional regulators (15, 18). IcaR was previously reported to repress *icaADBC* transcription by
123 binding to a 42-bp region within the *ica* promoter (16). The missense mutation that we identified
124 in *icaR* occurs in the HTH domain (Fig. S1 in the supplemental material) and may affect protein
125 function. Therefore, we complemented TF2758 with pC002, which is pKAT carrying *icaR* from
126 FK300. The resulting strain significantly decreased biofilm elaboration and PIA/PNAG produc-
127 tion was inhibited regardless of the presence or absence of glucose (Fig. 3A, B). These results
128 suggest that *icaR* from FK300 is functional and the *satf2583*-involved biofilm elaboration path-
129 way occurs through and upstream of the *ica* operon. We tentatively named this *orf* rob (regulator
130 of biofilm).

131 **Effects of Rob on biofilm elaboration, PIA/PNAG production, and *ica* operon expression in**
132 ***S. aureus* FK300.** TF2758 was resistant to transformation by the plasmid pKFT and pKOR1,

133 which are used for allelic exchange in *S. aureus*. Since the *rob* gene in FK300 is functional, we
134 selected strain FK300 for further studies on *rob* function. We introduced the same mutation
135 found in TF2758 into *rob* in FK300 by allelic replacement. As shown in Fig. 4A, this mutation in
136 *rob* resulted in a marked increase in biofilm elaboration in the presence or absence of 1% glucose.
137 The deletion of the *rob* gene also increased biofilm elaboration in FK300. We complemented the
138 *rob* deletion mutant with plasmids carrying the *rob* gene (SAOUHSC_2897) from FK300
139 (pC001) or the truncated *rob* gene (*satf2583*) from TF2758 (pC003). We found that the trans-
140 formant of the *rob* deletion mutant with pC001 exhibited repressed biofilm elaboration, similar
141 to the control, FK300. In contrast, pC003 was unable to complement the *rob* deletion phenotype,
142 which was similar to that of the *rob* deletion mutant carrying the mock vector pKAT (Fig. 4A).
143 In order to examine whether *rob* regulates biofilm elaboration through the *ica* operon, we
144 measured *icaR* and *icaADBC* expression by qRT-PCR and PIA/PNAG production in wild-type
145 and *rob* mutant strains of *S. aureus* FK300 (Fig. 4B). The results obtained indicated that the *rob*
146 deletion mutant decreased *icaR* expression and increased *icaADBC* expression with a concomi-
147 tant increase in PIA/PNAG production (Fig. 4C). The deletion of the *ica* operon in the FK300
148 *rob* deletion mutant abolished biofilm elaboration and PIA/PNAG production (Fig. 4A and C).
149 Taken together, these results suggest that biofilm elaboration in the *rob* deletion mutant is
150 *ica*-dependent and Rob, at least in part, represses *icaADBC* transcription.

151 **SAOUHSC_2898 (SATF2584) is involved in biofilm elaboration, which is under the control**

152 **of Rob.** The results of a preliminary microarray analysis suggested that Rob suppresses the ex-

153 pression of the surrounding 7-gene cluster (*satf2580-satf2586*) and the *ica* operon in TF2758

154 (Fig. 1C, Supple Table 1). Our RNA-seq data showed that these genes form operons (Fig. S2 in

155 the supplemental material). Therefore, we hypothesized that Rob affects biofilm elaboration by

156 repressing one or more genes in the (*satf2580-satf2586*) gene cluster. In order to test this possi-

157 bility, we deleted upstream genes (SAOUHSC_2894, SAOUHSC_2895) and downstream genes

158 (SAOUHSC_2898, SAOUHSC_2899 and SAOUHSC_2900) in the FK300 *rob* deletion mutant.

159 The results, shown in Figure 5, revealed that the deletion of the upstream genes had no signifi-

160 cant effect, whereas the deletion of the downstream genes significantly reduced biofilm elabora-

161 tion in the *rob* deletion mutant to a level similar to that of wild-type FK300.

162 As described above, there are three adjacent genes located immediately downstream of *rob*

163 that are under the control of one promoter forming an operon. We deleted each gene individually

164 in the FK300 *rob* deletion mutant (Fig. 6A). We found that only the SAOUHSC_2898 deletion

165 caused a marked reduction in biofilm elaboration. The SAOUHSC_2899 deletion had a slight

166 effect, whereas the SAOUHSC_2900 deletion had no effect on biofilm elaboration in the *rob*

167 deletion mutant. Additionally, biofilm elaboration could be restored through complementation of

168 *rob*, SAOUHSC_2898 double mutant with pC004, which carries the SAOUHSC_2898 gene

169 from FK300 (Fig. S3 in the supplemental material). These results suggest that SAOUHSC_2898
170 is a critical factor mediating biofilm elaboration regulated by Rob.

171 In order to further confirm the regulation of SAOUHSC_2898 by *rob*, qRT-PCR was per-
172 formed with RNA isolated from wild-type FK300 and the *rob* deletion mutant. The deletion of
173 *rob* resulted in the increased expression of SAOUHSC_2898 (Fig. 6B). SAOUHSC_2898 is pre-
174 dicted to encode a 2-deoxy-D-gluconate 3-dehydrogenase that belongs to the oxidoreductase
175 family (http://aureowiki.med.uni-greifswald.de/SAOUHSC_02898). Our results suggest that this
176 enzyme is involved in some unknown biosynthetic pathway impacting biofilm elaboration. Rob
177 may repress biofilm elaboration in FK300 by down-regulating the transcription of the SAOU-
178 HSC_2898 gene.

179 **Rob recognizes a palindromic motif in its own promoter.** A microarray analysis showed that
180 the inactivation of *rob* in TF2758 resulted in the increased expression of surrounding genes.
181 Therefore, using EMSA and DNase I footprint analyses, we investigated whether Rob directly
182 binds to its own promoter and regulates this gene cluster's transcription. We purified His-tagged
183 Rob from *E. coli* and its binding to an intergenic fragment between SAOUHSC_2896 and *rob*
184 (Fig. 7A). Rob induced significant dose-dependent shifts in the probe's mobility. A DNase I
185 footprint analysis clearly demonstrated that Rob bound to a 24-nucleotide DNA (Fig. 7B). We
186 then analyzed the secondary structure of the binding sequence. We found that it contained an al-
187 most perfect palindromic sequence (Fig. 7C). Interestingly, the transcription start site (TSS) of

188 *rob* was predicted to be within the binding region of Rob by RNA-sequencing (RNA-seq) analy-
189 sis (Fig. S2 in the supplemental material). These results suggest that Rob represses SAOU-
190 HSC_2898 transcription by recognizing the possible palindromic sequence present in the inter-
191 genic region of SAOUHSC_2896 and *rob*.

192 **Recombinant Rob binds to the *ica* promoter region.** As shown in Figure 4, the transcription
193 levels of *icaADBC* were also significantly increased in the *rob* mutant. In order to investigate
194 whether Rob directly modulates *icaADBC* expression by binding to the *ica* promoter, we used
195 EMSA to analyze the Rob protein binding to a 198-bp probe (FULL) that contained the entire
196 *icaR-icaA* intergenic region (Fig. 8A). As shown in Figure 8B, the recombinant Rob protein in-
197 duced several shifts, even with only 0.1 μg of FULL. Rob-DNA complex bands migrated in a
198 ladder-like pattern with increases in Rob protein concentrations. Rob-DNA complexes were out
199 competed with a 100-fold excess of unlabeled specific competitor DNA. These results suggest
200 that Rob binds to the *icaR-icaA* intergenic region in a dose-dependent manner.

201 Jefferson et al. previously identified a 5-bp (TATTT) motif within the *icaR-icaA* intergenic
202 region that controls the transcriptional regulation of the *ica* locus (16) (Fig. 8A). They suggested
203 that an unknown repressor(s) utilize(s) the TATTT sequence in order to regulate *icaADBC* ex-
204 pression. Since Rob represses the *ica* transcription of the *ica* locus, we investigated whether Rob
205 recognizes this 5-bp motif. We designed several additional probes for DNA binding assays (Fig.
206 8A). A 108-bp probe (SHORT-1), the shortest oligonucleotide containing the 5-bp sequence

207 lacking the 5' 90-bp sequence of FULL, was dose-dependently shifted by Rob (Fig. 8C). We then
208 generated an oligonucleotide (SHORT-2) with a 28-bp deletion from the 5' end of the SHORT-1
209 probe. As shown in Figure 8D, SHORT-2 had no significant shift in the presence of Rob. In order
210 to further investigate whether Rob recognizes the 5-bp motif, we made a 193-bp (FULL(- 5-bp))
211 probe lacking the 5-bp TATTT sequence of FULL. As shown in Figure 8E, FULL(- 5-bp) was
212 not shifted, as observed in FULL migration in Figure 8B, suggesting that Rob was unable to bind
213 to the 193-bp (FULL(- 5-bp)) probe. Taken together, these results suggest that Rob recognizes
214 and binds to the 5-bp motif within the *ica* promoter region.

215 We performed a DNase I footprint analysis to identify Rob-binding site(s). As shown in Fig-
216 ure 9, Rob protected a region of approximately 25 bp that included the 5-bp motif. In order to
217 further confirm that the 5-bp motif is necessary for the binding of Rob to the *icaR-icaA* intergen-
218 ic region, we attempted to screen for proteins bound to the *icaR-icaA* intergenic DNA fragment
219 with or without the 5-bp motif using cytosolic proteins of FK300. The cell extract of the
220 wild-type strain FK300 was mixed with magnetic beads conjugated with either the 198-bp
221 (FULL) probe or 193-bp (FULL(- 5-bp)) probe, and the bound proteins were then analyzed by
222 MALDI-TOF-MS. We found that Rob was present in proteins bound to the 198-bp probe, but
223 was absent in proteins bound to 193-bp (FULL(- 5-bp))(data not shown). Overall, these results
224 strongly suggest that Rob recognizes and binds to the 5-bp TATTT motif within the promoter re-
225 gion of the *ica* locus.

226

227 **DISCUSSION**

228 Biofilm elaboration is an important virulence determinant in certain types of *S. aureus*
229 infections, particularly those involving implanted medical devices. Biofilm growth is influenced
230 by a number of regulatory mechanisms. However, it is becoming increasingly apparent that the
231 transcriptional regulation of biofilm-associated genes, such as *icaADBC*, is complex. Staphylo-
232 coccal regulatory factors, including SarA, SigB, IcaR, TcaR, SrrAB, and Rbf, were previously
233 shown to regulate *icaADBC* expression (11, 15, 19-22). In the present study, we identified a nov-
234 el TetR/AcrR family regulator, Rob, which is a repressor of biofilm elaboration, by controlling
235 SAOUHSC_2898, within a 7-gene cluster under the control of Rob. Furthermore, we demon-
236 strated that Rob directly binds to the *icaR-icaA* intergenic region and represses *icaADBC*. The
237 binding site in the *icaR-icaA* intergenic region contained the 5-bp motif, which has been sug-
238 gested to control the transcriptional regulation of *icaADBC* (Fig. S4 in the supplemental materi-
239 al) (16).

240 The BLAST analysis showed that the *satf2580-satf2586* gene cluster, which was
241 up-regulated in the super biofilm-elaborating strain TF2758, is also present in several other
242 staphylococcal strains, but not in *S. epidermidis*, which is among the most studied and clinically
243 relevant biofilm-elaborating organisms (see Fig. S5 in the supplemental material). Therefore, a
244 novel regulatory pathway appears to be involved in biofilm elaboration in *S. aureus*.

245 SAOUHSC_2898 is predicted to encode a 2-deoxy-D-gluconate 3-dehydrogenase, which
246 belongs to the oxidoreductase family. Oxidoreductases specifically act on the CH-OH group of
247 donors with NAD+ or NADP+ as an acceptor. This enzyme participates in pentose and glucu-
248 ronate interconversions, a metabolic pathway that has recently been shown to be significantly
249 enriched in biofilm elaboration (23). An increase in the expression of oxidoreductase was previ-
250 ously reported to induce staphylococcal biofilm elaboration (24). The detailed characterization of
251 SAOUHC_2898 will provide an insight into *ica*-dependent biofilm elaboration.
252 SAOUHSC_2897 and SAOUHSC_2898 were previously reported to be accessory genes of a
253 glucose-induced biofilm designated as *gbaAB* (25). However, in our assay, the complementation
254 of TF2758 with SAOUHSC_2897 (*rob*) completely canceled PIA/PNAG production in the ab-
255 sence of 1% glucose. Furthermore, the addition of glucose did not alter the amount of
256 PIA/PNAG produced by the FK300 *rob* deletion mutant (Fig. 4C). Thus, it is reasonable to as-
257 sume that an SAOUHSC_2898-catalized pathway controlled by SAOUHSC_2897 (*rob*) affects
258 biofilm elaboration in a glucose-independent manner (Fig. 10).
259 A number of regulators, including SigB, SarA, and SarX, and two-component signal trans-
260 duction systems (TCSs) have been shown to affect staphylococcal biofilm elaboration (26-29).
261 Our genetic analyses showed that the deletion of *ica* genes or SAOUHSC_2898 resulted in a loss
262 in the ability to elaborate biofilms in the FK300 *rob* mutant. The *rob* mutant showed decreased

263 *icaR* expression and increased *icaADBC* transcription, suggesting that *rob* regulates an

264 *ica*-dependent pathway for biofilm elaboration, at least in part by activating *icaR* expression.

265 Some factors regulate *icaADBC* expression by binding to the *icaR-icaA* intergenic region

266 (15, 16, 22, 28). Although Rob is one of the TetR/AcrR family regulators in *S. aureus*, its role in

267 the regulation of biofilms is not completely clear. Jefferson et al. previously reported that the

268 TATTT sequence has a functional role in the transcriptional regulation of the *ica* locus (16). The

269 simple deletion of the TATTT motif in *S. aureus* MN8m markedly increased biofilm elaboration

270 and the transcription of *icaADBC*. They hypothesized the presence of uncharacterized re-

271 pressor(s) recognizing and binding to the motif. Most recently, Schwartbeck et al. also showed

272 that the *S. aureus* isolates carrying the 5-bp deletion exhibited a mucoid phenotype and strong

273 biofilm formation (30). These mucoid isolates were protected against phagocytosis and survived

274 better under starvation conditions. The results of the present study demonstrated that Rob binds

275 to an *icaR-icaA* intergenic region of approximately 25 bp including the 5-bp TATTT motif,

276 strongly suggesting that Rob is the postulated repressor reported by Jefferson et al. and further

277 support *rob* regulating biofilm elaboration in an *ica*-dependent manner. A comparison of the

278 Rob-binding site in the *icaR-icaA* intergenic region with that in the *rob* promoter revealed that

279 the right half of the palindrome sequence was also present in the *icaR-icaA* intergenic region (Fig.

280 9). This palindrome-like sequence may be recognized by Rob. A previous study showed that the

281 TATTT motif has a functional role in the transcriptional regulation of the *ica* locus, but not *icaR*

282 transcription (16). Ruiz de los Mozos et al. recently demonstrated that the 5'- and 3'- UTR base
283 pairings of *icaR* mRNA control its transcription in *S. aureus*. The 5-bp motif is located within the
284 5'-UTR of *icaR* (Fig. S4 in the supplemental material). The possibility of an interaction between
285 Rob and 5'-UTR to control base pairing remains elusive.

286 Taken together, the results of the present study suggest that Rob controls the two different
287 pathways of biofilm elaboration in *S. aureus*. The TetR-family transcriptional regulator Rob af-
288 fects biofilm elaboration through SAOUHSC_2898 and by recognizing/binding the TATTT motif
289 in an *ica*-dependent manner. These results provide additional insights into the transcriptional
290 regulation of the *ica* locus. Both Rob-mediated pathways will be investigated in more detail in
291 future studies.

292

293 **MATERIALS AND METHODS**

294 **Bacterial strains and growth media.** The bacterial strains and plasmids used in the present
295 study are listed in Table 1. The *S. aureus* strain, designated TF2758, is a clinical isolate from an
296 atheroma in Japan. *S. aureus* ATCC49775 served as a negative control, non-biofilm producer. *S.*
297 *aureus* FK300, a *rsbU*-repaired derivative of strain NCTC8325-4, was used in a functional study
298 of the role of *rob*. *S. aureus* RN4220 (31) was used as the initial recipient for the manipulation of
299 recombinant plasmids. *S. aureus* was routinely grown in tryptic soy broth (TSB, Becton Dickin-
300 son Microbiology Systems, Cockeysville, MD) or on tryptic soy agar (TSA) plates. Tetracycline

301 (Tc, 5 μg/ml) or chloramphenicol (Cp, 10 μg/ml) was added as necessary. *Escherichia coli* strain
302 DH5α was used for the construction and maintenance of plasmids. *E. coli* was grown in lysogeny
303 broth (LB) broth (5 g yeast extract, 10 g polypeptone, and 10 g NaCl per liter; pH 7.2) or on LB
304 agar. When required, ampicillin (Ap, 100 μg/ml), kanamycin (Kn, 30 μg/ml), Tc (10 μg/ml), or
305 Cp (10 μg/ml) was added to the culture medium.

306 **Plasmid and strain construction.** Routine DNA manipulations were performed as previously
307 described (32). FK300 mutants were constructed by allele replacement using pKFT (33). PCR
308 was performed using KOD-Plus-Neo (Toyobo, Japan) under appropriate cycling conditions. The
309 oligonucleotides used in this study are listed in Table 2. Fragments were cloned into the plasmid
310 pKFT using restriction enzymes and transformed into *E. coli* DH5α. Recombinant plasmids were
311 then introduced into DNA restriction system-deficient *S. aureus* RN4220 by electroporation (34).
312 Modified plasmids were electroporated into *S. aureus* FK300 for allele replacement. Markerless
313 deletion mutants were screened by PCR from tetracycline-sensitive colonies. Fragments were
314 confirmed by DNA sequencing using the BigDye Terminator v3.1 Cycle Sequencing Kit (Ap-
315 plied Biosystems, USA).

316 In complementation experiments, genes were amplified by PCR using the corresponding pri-
317 mer pairs and then cloned into the HindIII site of pKAT (35). The plasmids pC001, pC002, and
318 pC003 carrying *rob*-FK300, *icaR*-FK300, and *rob*-TF2758 genes, respectively, were constructed

319 and transformed into the *S. aureus* strains listed in Table 1 by electroporation. The inserts in all

320 plasmid constructs were verified by PCR and DNA sequencing.

321 **Biofilm assay.** A biofilm assay using polystyrene plates was performed as described previously

322 (36) with a few modifications. In brief, overnight cultures were diluted 1:100 with TSB. Ten mi-

323 croliters of this dilution was then transferred, in triplicate, into flat-bottom 96-well polystyrene

324 plates (TrueLine, Nippon Genetics Co., Ltd., Japan) containing TSB or TSB plus 1% glucose.

325 After incubation at 37°C for 24 h, the wells were gently washed three times with 300 µl of sterile

326 phosphate-buffered saline (PBS) (137 mM NaCl, 2.7 mM KCl, 10 mM $Na_2HPO_4 12H_2O$, and 1.8

327 mM KH_2PO_4, pH 7.4), and the biofilm was stained with 1% crystal violet for 15 min. Unbound

328 crystal violet was then removed by washing the plate in a container by immersing and agitating

329 gently 10 times in tap water. Biofilm-bound crystal violet was solubilized in 200 µl of 33% gla-

330 cial acetic acid at room temperature for 15 min. The extracts were diluted 10-fold, and absorb-

331 ance at 590 nm was measured with an Immuno-Mini NJ-2300 spectrophotometer (Nalge Nunc

332 International K.K., Tokyo, Japan).

333 **PIA/PNAG detection.** The ability of *S. aureus* strains to produce PIA/PNAG was tested ac-

334 cording to a previously described protocol (9). Briefly, *S. aureus* strains were grown at 37°C

335 overnight with shaking in 3 ml of TSB. Cultures were then diluted 1:1,000 in the appropriate

336 medium, and 4 ml of this cell suspension was used to inoculate sterile 12-well polystyrene plates

337 (TrueLine, Nippon Genetics Co., Ltd., Japan). After a 24-h static incubation at 37°C, the cells

338 were resuspended in 50 µl of 0.5 M EDTA (pH 8.0) and incubated for 5 min at 100°C. Cells
339 were removed by centrifugation, and 40 µl of the supernatant was incubated with 10 µl of pro-
340 teinase K (20 mg/ml; Nacalai Tesque, Inc., Kyoto, Japan) at 37°C for 30 min. After the addition
341 of 10 µl of Tris-buffer saline (20 mM Tris-HCl, 150 mM NaCl [pH 7.4]) containing 0.01% bro-
342 mophenol blue, 5 µl was immobilized on a nitrocellulose membrane (Amersham Protran NC
343 0.45, GE Healthcare, Buckinghamshire, UK) and dried at room temperature. The membrane was
344 blocked with 5% skimmed milk in PBS with 0.1% Tween 20, and this was followed by a 2-h in-
345 cubation with rabbit anti-PNAG antiserum (37) diluted at 1:10,000. Bound antibodies were de-
346 tected with peroxidase-conjugated goat anti-rabbit immunoglobulin G (IgG) antibodies (MP
347 Biomedicals, LLC-Cappel Products, Ohio, USA) diluted 1:10,000 and developed with Pierce
348 ECL Western Blotting Substrate (Thermo Scientific, Rockford, IL, USA).
349 **RNA isolation, reverse transcription (RT), and real-time PCR.** Overnight *S. aureus* cultures
350 were diluted in fresh TSB containing 1% glucose to an initial optical density of 0.02 at 660 nm
351 and harvested after a 6-h incubation with shaking at 37°C. Total RNA was isolated using the
352 FastRNA Pro Blue Kit (MP Biomedicals, LLC, Santa Ana, CA, USA) according to the manu-
353 facturer's instructions. DNA was removed by a treatment with RQ1 RNase-free DNase (Promega,
354 Madison, WI) at 37°C for 30 min. After inactivation of DNase, PCR was performed to confirm
355 the absence of contaminating DNA. RNA was then reverse transcribed with a Transcriptor First
356 Strand cDNA Synthesis Kit (Roche, Mannheim, Germany). The resulting cDNA was diluted

357 10-fold with Tris-EDTA (TE) buffer (10 mM Tris-HCl, 1 mM EDTA, pH 8.0) and then used as a
358 template in the real-time PCR reaction. Quantitative real-time RT-PCR (qRT-PCR) was per-
359 formed with the SsoAdvanced Universal SYBR Green Supermix (Bio-Rad, Hercules, CA, USA)
360 using a CFX96 Real-Time PCR Detection System (Bio-Rad). The thermal cycling conditions
361 used were as follows: at 95°C for 1 min, followed by 40 cycles of 95°C for 15 s, 60°C (*icaR* and
362 *icaA*) or 62°C (*gyrB* and SAOUHSC_2898) for 15 s, and 72°C for 30 s. All PCR runs were per-
363 formed in triplicate and data were analyzed using the CFX Manager Software (version 3.0,
364 Bio-Rad) according to the manufacturer's instructions. The housekeeping gene, gyrase subunit B
365 (*gyrB*), was used as a reference gene to normalize the expression level of the target gene in each
366 reaction. Real-time PCR primers are listed in Table 2.
367 **Microarray analysis.** The design and preparation of probes, which cover more than 98% of the
368 open reading frames (ORFs) of *S. aureus* MW2, and their immobilization on the glass slide were
369 described elsewhere (38). RNA extraction (after a 2-h incubation) and cDNA synthesis were
370 performed as described above. cDNA was fluorescently labeled with Alexa Fluor 555 (Cy3) and
371 Alexa Fluor 647 (Cy5) (Thermo Fisher Scientific, Oregon, USA). Labeled cDNA samples were
372 mixed and hybridized to the slides. After washing, fluorescent signals were detected using a
373 GenePix 4000B Microarray Scanner (Axon Instruments). Data were then normalized and ana-
374 lyzed using Array Vision 8.0 software (Imaging Research Inc., CT, USA). The

375 non-biofilm-elaborating strain ATCC49775, the genotype of which is the most closely related to

376 TF2758 in our Japanese clinical isolate collection, was used as the reference strain.

377 **Transcritomic analysis of *rob* operon via RNA-seq.**

378 Overnight *S. aureus* FK300 (wild-type, Δ*rob*) and TF2758 cultures were diluted in fresh TSB to

379 an initial density of 0.02 at 660 nm and harvested after a 6-h incubation with shaking at 37°C.

380 Total RNA was isolated using the FastRNA Pro Blue Kit (MP Biomedicals, LLC, Santa Ana, CA,

381 USA) according to the manufacturer's instructions. To eliminate DNA contamination, 1μg total

382 RNA in each sample was treated with 3 μl (1 U/μl) of RQ1 RNase-free DNase (Promega, Madi-

383 son, WI) at 37°C for 30 min. After digestion by DNase, PCR of the *gyrB* gene was performed to

384 confirm the absence of contaminating DNA. The concentration and quality of total RNA were

385 determined using a Qubit 2.0 Fluorometer (Thermo Fisher Scientific) and Agilent 2200 TapeSta-

386 tion (Agilent Techonogies), respectively. rRNA was removed using the Ribo-Zero Bacteria Kit

387 (Epicentre). Removal of rRNA was confirmed by Agilent 2200 TapeStation.

388 Libraries were generated using the ScriptSeq v2 RNA-Seq (Epicentre) and purified using the

389 Minelute PCR purification kit (Quiagen) according to the manufacturer's instructions. Libraries

390 were sequenced using the index sequences of TruSeq v2 LT Sample Prep Kit on the Illumina

391 MiSeq platform. Sequence reads were preprocessed for quality, trimmed and mapped to *S. aure-*

392 *us* strain NCTC8325 (GenBank accession number NC_007795) as the reference genome using

393 CLC Genomics Workbench software platform ver.9 (Qiagen) and Integrative Genomics Viewer

394 (IGV) ver.2.

395 **Sequencing of the TF2758 genome**. Genomic DNA was extracted using the lysostaphin and

396 QIAamp DNA Mini kit (QIAGEN, Germany) according to the manufacturer's instructions. Li-

397 braries were prepared for sequencing with Nextera DNA kits (Illumina, USA) and were se-

398 quenced with the Illumina GAIIx system according to Illumina protocols. The raw reads were

399 trimmed and assembled using a SOAPdenovo assembler. The draft genome sequence was auto-

400 matically annotated using the Microbial Genome Annotation Pipeline (MiGAP) (39) and was

401 manually curated using IMC-GE software (In Silico Biology, Inc., Kanagawa, Japan).

402 **Protein purification.** To elucidate the DNA-binding properties of Rob, the full-length open

403 reading frame (ORF) of *rob* was amplified from FK300 genomic DNA using primers

404 pET-28a-Rob-F/pET-28a-Rob-R (Table 2) and cloned into the expression vector pET-28a(+)

405 (Novagen) to obtain pET28a-*rob*. The plasmid was then transformed into *E. coli* BL21 (DE3)

406 and bacteria were grown at 37°C in 300 ml LB containing 30 μg/ml kanamycin to an OD of 0.5

407 at 600 nm. Expression of Rob was induced with 0.5 mM IPTG (isopro-

408 pyl-β-D-thiogalactopyranoside; Nacalai Tesque, Inc., Kyoto, Japan) and incubation at 37°C for

409 another 6 h. Cells were harvested by centrifugation and frozen at -80°C. Cell pellets were thawed

410 in lysis buffer (50 mM NaH_2PO_4 and 300 mM NaCl, pH 8.0) and lysed by sonication on ice. Cell

411 debris was removed by centrifugation (10,000 × *g* at 4°C for 20 min) and the supernatant was

412 used for isolation of His_6-tagged Rob fusion protein by using TALON Metal Affinity Resins
413 (Clontech Laboratories, Inc.) according to the company's protocol. The expression and purity of
414 the protein were analyzed by sodium dodecyl sulfate-polyacrylamide gel electrophoresis
415 (SDS-PAGE) using a 12% gel. Protein concentrations were measured using the Bio-Rad Protein
416 Assay (Bio-Rad, Hercules, CA) with bovine serum albumin (BSA) as the standard protein. The
417 recombinant His-tagged IcaR protein was purified as described elsewhere (18).
418 **Electrophoretic mobility shift assays (EMSA).** Gel shift assays were performed as described
419 previously (16) with the following modifications. DNA fragments corresponding to the *icaR-*
420 *icaA* intergenic region and promoter region of *rob* were amplified by PCR with the primers listed
421 in Table 2. PCR products were purified using the QIAquick Gel Extraction Kit (QIAGEN). A
422 20-μl binding reaction containing 0.1 to 2 μg of purified recombinant protein and 1 μg of soni-
423 cated salmon sperm DNA as well as 1 μg of poly(dI-dC) in binding buffer (10 mM Hepes [pH
424 8.0], 60 mM KCl, 4 mM $MgCl_2$, 0.1 mM EDTA [pH 8.0], 0.1 mg/ml BSA, 0.25 mM dithio-
425 threitol [DTT], and 5% glycerol) was incubated at room temperature for 15 min before the addi-
426 tion of 2 μg of the biotin-labeled probe. The reaction mixtures were incubated for an additional
427 20 min and then electrophoresed in 5% polyacrylamide gel in prechilled 1× Tris-borate-EDTA
428 (TBE) buffer. DNA was then transferred onto a nylon membrane (BioDyne B, PALL, USA) and
429 band shifts were detected by exposing dried membranes to X-ray films. In order to measure the

430 binding of Rob to its promoter region, a gel shift assay was performed using an alternative

431 method as described (40).

432 **DNase I footprint analysis.** Footprinting was performed according to a previously described

433 method (41). DNA fragments were generated by PCR with TaKaRa LA Taq (TaKaRa Bio Inc.,

434 Shiga, Japan). PCR products were purified and ligated with pGEM-T Easy (Promega) using Li-

435 gation high Ver.2 (Toyobo, Osaka, Japan). The resulting plasmids were then used as a template

436 for the amplification of DNA probes using the primer pair Fp-M13-F and Fp-M13-R

437 (5'-6-FAM-labeled). DNA fragments (0.45 pmol) were mixed with purified proteins in 50 µl of a

438 reaction mixture containing the same buffer used for gel shift assays. After a 20-min incubation

439 at room temperature, the reaction mixtures were treated with 0.3 U of DNase I (Promega, Madi-

440 son, WI) for 1 min and then purified by phenol/CIAA extraction and ethanol precipitation. After

441 purification, the samples were analyzed using an ABI 3130xl Genetic Analyzer equipped with

442 the Peak Scanner software (Applied Biosystems).

443 **Isolation and identification of proteins binding to the *ica* promoter.** A cell-free extract was

444 isolated from strain FK300 as previously described with some modifications (42). Briefly, cul-

445 tured *S. aureus* cells were pelleted and then washed with buffer A (20 mM Tri-HCl, 5 mM $MgCl_2$,

446 0.1 M EDTA, and 5% glycerol, pH 7.8). Cell pellets were resuspended in 10 ml of buffer A and

447 treated with lysostaphin (0.1 mg/ml) at 4°C for 1 h. After freezing at -80°C and thawing at 4°C

448 twice, 6 ml of buffer A (containing KCl at a final concentration of 1.3 M) was added and incu-

449 bated on ice for 40 min. The cell lysate was treated with DNase I (10 μg/ml) and RNase A (10

450 μg/ml) at room temperature for 30 min. After centrifugation for 30 min at 40,000 × *g*, the su-

451 pernatant was dialyzed against distilled water overnight and stored at -80°C.

452 Biotinylated DNA was prepared as described above. DNA was immobilized on 2 mg of

453 streptavidin-coated magnetic beads (Dynabeads M-280 Streptavidin; Life Technologies) accord-

454 ing to the manufacturer's protocol. After washing, 100 μl of the cell-free extract was added and

455 incubated at room temperature for 30 min in gel shift binding buffer. The beads were washed

456 twice with buffer B (10 mM Hepes [pH 8.0], 60 mM KCl, 4 mM $MgCl_2$, 1 mM EDTA [pH 8.0],

457 1 mM DTT, and 5% glycerol) containing 0.5 μg/ml of salmon sperm DNA, and then washed

458 twice with buffer B. The bound proteins were eluted from immobilized DNA with buffer B con-

459 taining 0.5 M NaCl. The eluates from two binding reactions were pooled and concentrated by

460 methanol/chloroform precipitation. Proteins were separated by SDS-PAGE, followed by Coo-

461 massie or silver staining. Prior to in-gel trypsin digestion, excised gel pieces were destained

462 and submitted to reduction with DTT and alkylation with iodoacetamide as described previously

463 (43). After being dried, the gel pieces were subjected to trypsin digestion at 35°C overnight with

464 XL-TrypKit (APRO Sci, Japan). Digested peptides were transferred to new tubes and evaporated

465 to < 10 μl in a vacuum centrifuge evaporator, and this was followed by LC-MS/MS analyses for

466 protein identification. LC-MS/MS analyses were performed on nanoflow liquid chromatography

467 coupled with nanoelectrospray MS, a Triple TOF 5600 system (AB SCIEX, CONCORD, ON)

468 equipped with an Eksigent cHiPLC-nanoflex System (AB SCIEX). The nano HPLC columns
469 used were the cHiPLC trap column (200 µm x 0.5 mm ChromXP C18-CL, 3 µm) and nano
470 cHiPLC analytical capillary column (75 µm x 15 cm ChromXP C18-CL, 3 µm, 120Å). Tryptic
471 peptides (2 µl) were loaded, and trapping and desalting were performed at 2 µl/min for 10 min
472 with 0.1% formic acid. The trapped peptides were separated by a linear gradient at a flow rate of
473 0.3 µl/min, followed by their introduction into the source of the mass spectrometer online. Mo-
474 bile phase A (0.1% formic acid in H_2O) and mobile phase B (0.1% formic acid in acetonitrile)
475 were used to establish a 45-min gradient comprising 25 min of 2-32% B, 1 min of 32-90% B, 4
476 min of 90% B, and finally decreasing to 2% B, which was followed by re-equilibrating at 2% B
477 for 15 min. Eluted peptides from the column were analyzed with a Triple TOF 5600 using an ion
478 spray voltage of 2.2kV. Product ions were scanned in a mass range from 230m/z up to 1500 m/z.
479 MS/MS data acquisition was performed using Analyst 1.5.2 (AB Sciex) and proteins were iden-
480 tified by means of an automated database search using ProteinPilot Software (AS Sciex).
481

482 **SUPPLEMENTAL MATERIAL**

483 Supplemental material for this article may be found at:
484 Table S1
485 Figure S1
486 Figure S2

487 Figure S3

488 Figure S4

489 Figure S5

490 **ACKNOWLEDGMENTS**

491 We thank Dr. Hidetada Hirakawa, Gunma Univ. for his skillful suggestion on DNase I footprint

492 analysis. This work is supported in part by a grant from the Health and Labor Sciences Research

493 Grants for Research on Allergic Disease and Immunology from the Ministry of Health, Labor,

494 and Welfare of Japan (201322025A), and a grant from the Japan Agency for Medical Research

495 and Development (AMED) (924711).

496

497 **REFERENCES**

498 1. **Donlan, R. M., and J. W. Costerton.** 2002. Biofilms: survival mechanisms of clinically

499 relevant microorganisms. Clin Microbiol Rev **15:**167–193.

500 2. **Mayberry-Carson, K. J., B. Tober-Meyer, J. K. Smith, D. W. Lambe, Jr., and J. W.**

501 **Costerton.** 1984. Bacterial adherence and glycocalyx formation in osteomyelitis experimen-

502 tally induced with *Staphylococcus aureus*. Infect Immun **43:**825–833.

503 3. **Götz, F.** 2002. *Staphylococcus* and biofilms. Mol Microbiol **43:**1367–1378.

504 4. **Otto, M.** 2008. Staphylococcal biofilms. Curr Top Microbiol Immunol **322:**207–228.

505 5. **Lister J, Horswill A.** 2014. *Staphylococcus aureus* biofilms: recent developments in biofilm
506 dispersal. Front Cell Infect Microbiol **4:**178.
507 6. **Jones SM, Morgan M, Humphrey TJ, Lappin-Scott H.** 2001. Effect of vancomycin and
508 rifampicin on meticillin-resistant *Staphylococcus aureus* biofilms. Lancet **357:**40–41.
509 7. **Otto M.** 2013. Staphylococcal infections: mechanisms of biofilm maturation and detachment
510 as critical determinants of pathogenicity. Annu Rev Med **64:**175–188.
511 8. **Mack, D., Fischer, W., Krokotsch, A., Leopold, K., Hartmann, R., Egge, H., and Laufs,**
512 **R.** 1996. The intercellular adhesin involved in biofilm accumulation of *Staphylococcus epi-*
513 *dermidis* is a linear beta-1,6-linked glucosaminoglycan: purification and structural analysis. J
514 Bacteriol **178:**175–183.
515 9. **Cramton, S. E., C. Gerke, N. F. Schnell, W. W. Nichols, and F. Götz.** 1999. The intercel-
516 lular adhesion (*ica*) locus is present in *Staphylococcus aureus* and is required for biofilm
517 formation. Infect Immun **67:**5427–5433.
518 10. **Heilmann C., Schweitzer O., Gerke C., Vanittanakom N., Mack D., Götz F.**
519 1996. Molecular basis of intercellular adhesion in the biofilm-formation *Staphylococcus epi-*
520 *dermidis*. Mol Microbiol **20:**1083–1091.
521 11. **Lim Y, Jana M, Luong TT, Lee CY.** 2004. Control of glucose- and NaCl-induced biofilm
522 formation by *rbf* in *Staphylococcus aureus*. J Bacteriol **186:**722–729.

523 12. **Dobinsky S, Kiel K, Rohde H, Bartscht K, Knobloch JK, Horstkotte MA, Mack D.** 2003.
524 Glucose-related dissociation between *icaADBC* transcription and biofilm expression
525 by *Staphylococcus epidermidis*: evidence for an additional factor required for polysaccharide
526 intercellular adhesin synthesis. J Bacteriol **185:**2879–2886.
527 13. **Knobloch JK, Bartscht K, Sabottke A, Rohde H, Feucht HH, Mack D.** 2001. Biofilm
528 formation by *Staphylococcus epidermidis* depends on functional RsbU, an activator of the
529 *sigB* operon: differential activation mechanisms due to ethanol and salt stress. J Bacteriol
530 **183:**2624–2633.
531 14. **Cramton SE, Ulrich M, Götz F, Doring G.** 2001. Anaerobic conditions induce expression
532 of polysaccharide intercellular adhesin in *Staphylococcus aureus* and *Staphylococcus epi-*
533 *dermidis*. Infect Immun **69:**4079–4085.
534 15. **Conlon, K. M., Humphreys, H., and O'Gara, J. P.** 2002. *icaR* encodes a transcriptional
535 repressor involved in environmental regulation of *ica* operon expression and biofilm for-
536 mation in *Staphylococcus epidermidis*. J Bacteriol **184:**4400–4408.
537 16. **Jefferson, K. K., S. E. Cramton, F. Götz, and G. B. Pier.** 2003. Identification of a
538 5-nucleotide sequence that controls expression of the *ica* locus in S*taphylococcus aureus* and
539 characterization of the DNA-binding properties of IcaR. Mol Microbiol **48:**889–899.

540 17. **Shrestha, L., Kayama, S., Sasaki, M., Kato, F., Hisatsune, J., Tsuruda, K., Koizumi, K.,**
541 **Tatsukawa, N., Yu, L., Takeda, K. and Sugai, M.** 2016. Inhibitory effects of antibiofilm
542 compound 1 against *Staphylococcus aureus* biofilms. Microbiol and Immunol **60:**148–159.
543 18. **Jeng WY, Ko TP, Liu CI, Guo RT, Liu CL, Shr HL, Wang AH.** 2008. Crystal structure of
544 IcaR, a repressor of the TetR family implicated in biofilm formation in *Staphylococcus epi-*
545 *dermidis*. Nucleic Acids Res **36:**1567–1577.
546 19. **Ulrich, M., M. Bastian, S. E. Cramton, K. Ziegler, A. A. Pragman, A. Bragonzi, G.**
547 **Memmi, C. Wolz, P. M. Schlievert, A. Cheung, and G. Doring.** 2007. The staphylococcal
548 respiratory response regulator SrrAB induces *ica* gene transcription and polysaccharide in-
549 tercellular adhesin expression, protecting *Staphylococcus aureus* from neutrophil killing un-
550 der anaerobic growth conditions. Mol Microbiol **65:**1276–1287.
551 20. **Valle, J., A. Toledo-Arana, C. Berasain, J. M. Ghigo, B. Amorena, J. R. Penades, and I.**
552 **Lasa.** 2003. SarA and not sigmaB is essential for biofilm development by *Staphylococcus*
553 *aureus*. Mol Microbiol **48:**1075–1087.
554 21. **Cue D, Lei MG, Luong TT, Kuechenmeister L, Dunman PM, O'Donnell S, Rowe S,**
555 **O'Gara JP, Lee CY.** 2009. Rbf promotes biofilm formation by *Staphylococcus aureus* via
556 repression of *icaR*, a negative regulator of *icaADBC*. J Bacteriol **191:**6363–6373.
557 22. **Jefferson, K. K., D. B. Pier, D. A. Goldmann, and G. B. Pier.** 2004. The
558 teicoplanin-associated locus regulator (TcaR) and the intercellular adhesin locus regulator

559 (IcaR) are transcriptional inhibitors of the *ica* locus in *Staphylococcus aureus*. J Bacteri-
560 ol **186:**2449–2456.
561 23. **Li Z, Chen Y, Liu D, Zhao N, Cheng H, Ren H, Guo T, Niu H, Zhuang W, Wu J, Ying H.**
562 2015. Involvement of glycolysis/gluconeogenesis and signaling regulatory pathways in *Sac-*
563 *charomyces cerevisiae* biofilms during fermentation. Front Microbiol **6:**139.
564 24. **Kulkarni R, Antala S, Wang A, Amaral FE, Rampersaud R, Larussa SJ, Planet PJ,**
565 **Ratner AJ.** 2012. Cigarette smoke increases *Staphylococcus aureus* biofilm formation via
566 oxidative stress. Infect Immun **80:**3804–3811.
567 25. **You Y, Xue T, Cao L, Zhao L, Sun H, Sun B.** 2014. *Staphylococcus aureus* glu-
568 cose-induced biofilm accessory proteins, GbaAB, influence biofilm formation in a
569 PIA-dependent manner. Int J Med Microbiol **304:**603-612.
570 26. **Lauderdale KJ, Boles BR, Cheung AL, Horswill AR.** 2009. Interconnections between
571 Sigma B, *agr*, and proteolytic activity in *Staphylococcus aureus* biofilm maturation. Infect
572 Immun **77:**1623–1635.
573 27. **Tormo MA, Marti M, Valle J, Manna AC, Cheung AL, Lasa I, Penades JR.** 2005. SarA
574 is an essential positive regulator of *Staphylococcus epidermidis* biofilm development. J Bac-
575 teriol **187:**2348–2356.
576 28. **Cue D, Lei MG, Lee CY.** 2013. Activation of *sarX* by Rbf is required for biofilm formation
577 and *icaADBC* expression in *Staphylococcus aureus*. J Bacteriol **195:**1515–1524.

578 29. **Sharma-Kuinkel BK, Mann EE, Ahn JS, Kuechenmeister LJ, Dunman PM, Bayles KW.**
579 2009. The Staphylococcus aureus LytSR two-component regulatory system affects biofilm
580 formation. J Bacteriol **191:**4767–4775.
581 30. **Schwartbeck B, Birtel J, Treffon J, Langhanki L, Mellmann A, Kale D, et al.** 2016. Dy-
582 namic in vivo mutations within the *ica* operon during persistence of *Staphylococcus aureus*
583 in the airways of cystic fibrosis patients. PLoS Pathog **12 (11)**:e1006024.
584 31. **Kreiswirth, B. N., S. Lofdahl, M. J. Betley, M. O'Reilly, P. M. Shlievert, M. S. Bergdoll,**
585 **and R. P. Novick.** 1983. The toxic shock syndrome exotoxin structural gene is not detectably
586 transmitted by a prophage. Nature **305:**709–712.
587 32. **Sambrook, J., Fritsch, E.F., Maniatis, T.** 1989. Molecular cloning: a laboratory manual.
588 Cold Spring Harbor Laboratory Press, Plain View, NY.
589 33. **Kato F, Sugai M.** 2011. A simple method of markerless gene deletion in *Staphylococcus au-*
590 *reus*. J Microbiol Methods **87:**76–81.
591 34. **Kraemer, G. R., and J. J. Iandolo.** 1990. High-frequency transformation of *Staphylococcus*
592 *aureus* by electroporations. Curr Microbiol **21:**373–376.
593 35. **Kato, F.** 2004. Ph.D. thesis, University of Tohoku, Sendai, Japan. NDLC:UT51-2004-P732.
594 36. **Heilmann, C., Gerke, C., Perdreau-Remington, F., and Götz, F.** 1996. Characterization of
595 Tn917 insertion mutants of *Staphylococcus epidermidis* affected in biofilm formation. Infect
596 Immun **64:**277–282.

597 37. **Skurnik D, Merighi M, Grout M, Gadjeva M, Maira-Litran T, Ericsson M, Goldmann**
598 **DA, Huang SS, Datta R, Lee JC, Pier GB.** 2010. Animal and human antibodies to distinct
599 *Staphylococcus aureus* antigens mutually neutralize opsonic killing and protection in mice. J
600 Clin Invest **120:**3220–3233.
601 38. **Aburatani S, Tashiro K, Savoie CJ, Nishizawa M, Hayashi K, Ito Y, Muta S, Yamamoto**
602 **K, Ogawa M, Enomoto A, Masaki M, Watanabe S, Maki Y, Takahashi Y, Eguchi Y, Sa-**
603 **kaki Y, Kuhara S.** 2003. Discovery of novel transcription control relationships with gene
604 regulatory networks generated from multiple-disruption full genome expression libraries.
605 DNA Res **10:**1-8.
606 39. **Sugawara H, Ohyama A, Mori H and Kurokawa K.** 2009. "Microbial Genome Annota-
607 tion Pipeline (MiGAP) for diverse users" The 20th International Conference on Genome In-
608 formatics (GIW2009) Poster and Software Demonstrations (Yokohama), S001-1-2.
609 40. **Sato'o Y, Hisatsune J, Nagasako Y, Ono HK, Omoe K, Sugai M.** 2015. Positive regulation
610 of staphylococcal enterotoxin H by Rot (repressor of toxin) protein and its importance in
611 clonal complex 81 subtype 1 lineage-related food poisoning. Appl Environ Microbiol
612 **81:**7782–7790.
613 41. **Hirakawa H, Y. Oda, S. Phattarasukol, C. D. Armour, J. C. Castle, C.K. Raymond, C. R.**
614 **Lappala, A. L. Schaefer, C. S. Harwood and E. P. Greenberg.** 2011. Activity of the Rho-

615 dopseudomonas palustris p-coumaroyl-homoserine lactone responsive transcription factor
616 RpaR. J Bacteriol **193:**2598–2607.
617 42. **Oscarsson, J., C. Harlos, and S. Arvidson.** 2005. Regulatory role of proteins binding to the
618 *spa* (protein A) and *sarS* (staphylococcal accessory regulator) promoter regions in *Staphylo-*
619 *coccus aureus* NTCC 8325-4. Int. J. Med. Microbiol. **295:**253-266.
620 43. **Hara K, Ohara M, Hayashi I, Hino T, Nishimura R, Iwasaki Y, Ogawa T, Ohyama Y,**
621 **Sugiyama M, Amano H.** 2012. The green tea polyphenol (-)-epigallocatechin gallate precip-
622 itates salivary proteins including alpha-amylase: biochemical implications for oral health.
623 Eur J Oral Sci **120**:132-139.
624 44. **Ruiz de los Mozos I, Vergara-Irigaray M, Segura V, Villanueva M, Bitarte N, Saramago**
625 **M, Domingues S, Arraiano CM, Fechter P, Romby P, Valle J, Solano C, Lasa I, Tole-**
626 **do-Arana A.** 2013. Base pairing interaction between 5'- and 3'-UTRs controls *icaR* mRNA
627 translation in *Staphylococcus aureus*. PLoS Genet **9(12)**:e1004001.
628 45. **Cue D, Lei MG, Lee CY.** 2012. Genetic regulation of the intercellular adhesion locus in
629 staphylococci. Front Cell Infect Microbiol **2:**38.
630

631 **Figure legends**

632 **FIG. 1 Biofilm elaboration and PIA/PNAG production by *Staphylococcus aureus* TF2758.**
633 (A) Biofilm elaboration. Bacteria were grown in trypticase soy broth (TSB) in the presence

634 (Glc+) or absence (Glc-) of 1% glucose. Biofilm elaboration was measured using the polystyrene
635 microtiter plate assay described in the Materials and Methods section. The averages and standard
636 errors from each sample are shown. (B) PIA/PNAG production. Extracts from overnight cultures
637 were spotted on a membrane, and PIA/PNAG was detected by rabbit anti-PNAG, as described in
638 the Materials and Methods section. Non-biofilm-elaborating strain ATCC49775 was used as a
639 control in the comparative microarray analysis. (C) A comparative gene expression analysis of
640 TF2758 and ATCC49775. TF2758 gene expression was represented as fold changes from that of
641 ATCC49775. Two gene clusters exhibiting marked increases in gene expression were colored
642 (red and blue), and these gene clusters were depicted (a, b).
643
644 **FIG. 2 Identification of a nonsense mutation in the *satf2583* (*rob*) gene of TF2758 and the**
645 **predicted domain structure of its transcript.** (A) Comparison of the *satf2580-satf2586* region
646 with those of MW2, 8325-4, ATCC49775, and TF2758. A part of the nucleotide sequence of each
647 strain and amino acid sequences are shown. The numbers shown on both sides mean the nucleo-
648 tide sequence and amino acid sequence positions in the ORF of *rob*. The nonsense codon created
649 by the mutation (A to T) was indicated by an asterisk. (B) Structural characteristics of Rob. It
650 contained a TetR_N superfamily domain within an AcrR domain.
651

652 **FIG. 3 Rob and IcaR from FK300 reduce biofilm elaboration and PIA/PNAG synthesis in**

653 **strain TF2758.** (A) Biofilm elaboration and (B) PIA/PNAG production of TF2758 and TF2758

654 carrying pC001 (pKAT-*rob* (FK300)), pC002 (pKAT-*icaR* (FK300)), or pKAT. Bacteria were

655 grown TSB in the presence (Glc+) or absence (Glc-) of 1% glucose. Biofilm elaboration was

656 measured using the polystyrene microtiter plate assay described in the Materials and Methods

657 section. The averages and standard errors from each sample are shown. Extracts from overnight

658 cultures were spotted on a membrane, and PIA/PNAG was detected by rabbit anti-PIA, as de-

659 scribed in the Materials and Methods section.

660

661 **FIG. 4 Effects of the *rob* deletion on biofilm elaboration and *ica* operon expression in**

662 **FK300.** (A) Biofilm elaboration in wild-type FK300 and its derivatives were assessed using the

663 polystyrene microtiter plate assay described in the Materials and Methods section. The averages

664 and standard errors from each sample are shown. sm, FK300 carrying a stop mutation at adenine

665 nucleotide position 331(A_{331} to T_{331}); pC001, pKAT with *rob* (FK300); pC003, pKAT with *rob*

666 (TF2758). (B) Quantitative measurements of *icaR* and *icaADBC* transcription by qPCR. Total

667 RNA preparation, cDNA synthesis, and then qPCR were performed as described in the Materials

668 and Methods section. Transcript levels in the *rob* deletion mutant compared to those in wild-type

669 strain FK300 were assigned. The expression of the *gyrB* gene was used for sample normalization.

670 Error bars indicate standard errors. (C) PIA/PNAG production. PIA/PNAG production was

671 measured as described in the legend of Figure 1.

672

673 **FIG. 5 Biofilm elaboration in the *rob* deletion mutant requires downstream gene(s), but not**

674 **upstream genes.** Bacteria were grown in TSB in the presence (Glc+) or absence (Glc-) of 1%

675 glucose. Biofilm elaboration was measured using the polystyrene microtiter plate assay de-

676 scribed in the Materials and Methods section. The averages and standard errors from each sam-

677 ple are shown. Δ*rob,* FK300 *rob* deletion mutant; Δ*rob*ΔUpstream, FK300 with deletions of *rob*

678 and its upstream genes, SAOUHC_ 2894, SAOUHC_ 2895, and SAOUHSC_2896;

679 Δ*rob*ΔDownstream, FK300 with the deletion of *rob* and its downstream genes SAOUHSC_2898,

680 SAOUHSC_2899, and SAOUHSC_2900.

681

682 **FIG. 6 Contribution of SAOUHSC_2898 to biofilm elaboration by the *rob* deletion mutant**

683 **and regulation of SAOUHSC_2898 expression by *rob* in FK300.** Bacteria were grown in TSB

684 in the presence (Glc+) or absence (Glc-) of 1% glucose. Biofilm elaboration was measured using

685 the polystyrene microtiter plate assay described in the Materials and Methods section. (A) Ef-

686 fects of SAOUHSC_2898, SAOUHSC_2899, and SAOUHSC_2900 deletions on biofilm elabo-

687 ration in the FK300 *rob* deletion mutant. The averages and standard errors from each sample are

688 shown. (B) Transcription of SAOUHSC_2898 in the FK300 wild-type strain and its *rob* deletion

689 mutant. Transcript levels in the *rob* deletion mutant compared to those in the wild-type strain

690 were assigned. The expression of the *gyrB* gene was used for sample normalization. Error bars

691 indicate standard errors.

692

693 **FIG. 7 Rob binds to a palindromic motif in its own promoter.** (A) EMSA for the

694 DNA-binding activity of Rob to the intergenic region between SAOUHSC_2896 and *rob*. EMSA

695 was performed in the absence (lane 1) or presence (lanes 2 to 5) of the Rob protein. The primers

696 used to amplify the intergenic region for Rob binding are indicated by black arrows. (B) DNase I

697 footprinting assay. The 6-FAM-labeled DNA probe was incubated with or without recombinant

698 Rob (12 pmol) and then subjected to DNase I digestion. The rectangle indicates the region pro-

699 tected by Rob. The palindromic motif is shown in bold. (C) Schematic representation of the sec-

700 ondary structure of the binding region by Rob. The sequence bound by Rob is highlighted by a

701 red frame.

702

703 **FIG. 8 Rob binds to the *ica* promoter region and its binding is TATTT motif-dependent.**

704 (A) Schematic representation of the design of DNA probes used in EMSAs. (B-E) EMSAs of

705 Rob. Recombinant Rob was incubated with (B) FULL, (C) SHORT-1, (D) SHORT-2, or (E)

706 FULL (-5-bp) (2 ng/reaction). The amounts (μg/reaction) of Rob were as follows: (B-E) lane 1,

707 0; lanes 2 to 5 were 0.1, 0.5, 1.0, and 1.5, respectively. (B) lane 6, 1.5 (with 100–fold excess of

708 unlabeled specific competitor). (C-E) lane 6, 2.0.

709

710 **FIG. 9 DNase I footprinting assay of Rob binding to the *ica* promoter region.** (A) A footprint

711 analysis of Rob binding to the *ica* promoter region. The sequence of the protected region is

712 shown. (B) Comparison of the binding sites of Rob to the *rob* promoter region and *ica* promoter

713 region. The palindromic sequence within the Rob binding region is shaded. The bold letters (A)

714 and rectangle (B) indicate the 5-bp TATTT motif.

715

716 **Fig. 10 Proposed model for the regulation of PIA/PNAG synthesis by Rob in *S. aureus***

717 **FK300.** The *rob* gene product represses the expression of the surrounding 7-gene cluster includ-

718 ing *rob* and SAOUHSC_2988. The gene product of SAOUHSC_2988 may function as an oxi-

719 doreductase in a hypothetical pathway through which glucose-independent *icaADBC*-dependent

720 polysaccharide accumulation occurs. *rob* also recognizes the TATTT motif in the *ica* promoter

721 region and binds to this region. The binding of Rob to the *ica* promoter region may suppress the

722 expression of the *icaADBC* locus. 5-bp, the TATTT motif important for the expression of *ica* lo-

723 cus. 42-bp, the IcaR-binding region. Arrows correspond to activation and bars to repression.

724

725 **FIG. S1 Identification of a missense mutation in the *icaR* gene of TF2758 and the domain**

726 **structure of its transcript.** (A) Comparison of the nucleotide sequence and amino acid se-

727 quence of the *icaR* gene among MW2, 8325-4, ATCC49775, and TF2758. The numbers shown

728 on both sides mean the nucleotide sequence and amino acid sequence positions in the ORF of

729 *icaR*. Altered amino acids (A to T) by the mutation at nucleotide position 103 (G to A) were in-

730 dicated in red. (B) Structural characteristics of IcaR. It contained a TetR_N superfamily domain

731 within an AcrR domain.

732

733 **FIG. S2 Identification of *rob* operon and transcription start site of *rob* using RNA-seq**

734 **analysis.** (A) Visualization of RNA transcript identified by RNA-seq. Total RNA of FK300,

735 FK300 Δ*rob*, and TF2758 were prepared from cultures grown for 6 h at 37°C. After removal of

736 DNA contaminants and rRNA, libraries were generated and purified as described in the Materi-

737 als and Methods. RNA-seq reads were mapped to *S. aureus* NCTC8325. Genes with continuous

738 coverage were considered to belong to the same operon. The ORFs of NCTC8325 are shown at

739 the top of the figure. Transcripts identified by RNA-seq are represented as dashed arrows. The

740 sequence from predicted transcription start site (TSS) to the start codon of *rob* was shown at the

741 bottom of the figure. (B) Diagrammatic representation of the *rob* promoter region.

742 GENETYXMAC v.15 (Software Development Co., Ltd., Tokyo, Japan) was used for prediction

743 of the -35, -10 sequence. The start codons of genes are indicated by arrows. The Rob-binding site

744 is indicated by the open rectangle. The transcription start site of *rob* is highlighted by a bent ar-

745 row.

746

747 **FIG. S3 Reduced biofilm elaboration in *rob* SAOUHSC_2898 double mutant was restored**

748 **through complementation with the SAOUHSC_2898 gene.** Bacteria were grown in TSB in

749 the presence (Glc+) or absence (Glc-) of 1% glucose. Biofilm elaboration was measured using

750 the polystyrene microtiter plate assay described in the Materials and Methods section. The aver-

751 ages and standard errors from each sample are shown. pC004, pKAT with SAOUHSC_2898

752 (FK300).

753

754 **FIG. S4 Diagrammatic representation of the *icaR-icaA* intergenic region.** The start sites of

755 *icaR* and *icaA* are indicated by arrows. The Rob-binding site is indicated by the open rectangle.

756 The grey shaded rectangle indicates the IcaR-binding site (16). The 5-bp TATTT motif, which

757 has a functional role in the transcriptional regulation of the *ica* locus, is highlighted by a red

758 frame (16). The Shine-Dalgarno sequence of *icaR* is underlined. The 5'-UTR of *icaR* is boxed

759 (dashed line) in the sequence (44). The bent arrow indicates the transcriptional start site of *icaA*

760 (45).

761

762 **FIG. S5 Comparison of the *satf2580-satf2586* region among different staphylococcus spe-**

763 **cies.** The red frame represents the 7-gene cluster highlighted in this study.

764

765

766 **TABLE 1** Strains and plasmids used in the present study

Strain or plasmid	Relevant characteristic(s)	Source or reference
Strains		
S. aureus		
TF2758	Wild-type clinical isolate, biofilm-positive	This study
ATCC49775	Wild-type clinical isolate, biofilm-negative	ATCC
FK300	Derivative of NCTC8325-4 (*rsbU* repaired)	Laboratory stock
RN4220	Restriction-negative strain, NCTC8325-4 derivative	31
TF2758 pC001	TF2758 complemented with pC001	This study
TF2758 pC002	TF2758 complemented with pC002	This study
rob_{sm}	FK300 with a stop mutation in *rob*	This study
Δ*rob*	FK300 Δ*rob*	This study
Δ*rob* pC001	FK300 Δ*rob* complemented with pC001	This study
Δ*rob* pC003	FK300 Δ*rob* complemented with pC003	This study
Δ*rob* pKAT	FK300 Δ*rob* complemented with pKAT	This study
Δ*rob* Δ*icaADB*	FK300 Δ*rob* Δ*icaADB*	This study
Δ*rob* ΔUpstream	FK300 Δ*rob* ΔSAOUHSC_2894 ΔSAOUHSC_2895 ΔSAOUHSC_2896	This study
Δ*rob* ΔDownstream	FK300 Δ*rob* ΔSAOUHSC_2898 ΔSAOUHSC_2899 ΔSAOUHSC_2900	This study
Δ*rob* ΔSAOUHSC_2898	FK300 Δ*rob* ΔSAOUHSC_2898	This study
Δ*rob* ΔSAOUHSC_2899	FK300 Δ*rob* ΔSAOUHSC_2899	This study
Δ*rob* ΔSAOUHSC_2900	FK300 Δ*rob* ΔSAOUHSC_2900	This study
E. coli		
DH5α	Cloning strain	TaKaRa
BL21(DE3)	Host for recombinant protein production	Novagen
Plasmids		
pGEM-T Easy	Cloning vector	Promega
pKAT	*E. coli-S. aureus* shuttle vector	35
pC001	Vector for complementation experiments; containing *rob* from FK300 cloned in pKAT	This study

pC002	Vector for complementation experiments; containing *icaR* from FK300 cloned in pKAT	This study
pC003	Vector for complementation experiments; containing *rob* from TF2758 cloned in pKAT	This study
pC004	Vector for complementation experiments; containing SAOUHSC_2898 from FK300 cloned in pKAT	This study
pKFT	Vector for allele replacement	33
pET-28a(+)	*E. coli* expression plasmid	Novagen
pET-22b(+)	*E. coli* expression plasmid	Novagen
pET28a-*rob*	His-Rob expression plasmid	This study
pET22b-*icaR*	His-IcaR expression plasmid	This study

767

768 **TABLE 2** Primers used in the present study

Primer	Sequence (5'-3')
Plasmid and strain construction	
rob_{sm}-1	ACAACGCCCTTAATTGTTGCC
rob_{sm}-2	GCAACAATTAAGGGCGTTGTTACCAAAG
rob-1	TACCAAGCTTCCTCTAACAACTGTTTTAC
rob-2	CATCAACTAGTTTGTGCGCTATTTCTTC
rob-3	GCTGTTGCAATCATTATCAACTAGTG
rob-4	AGGTAAAGCTTTAGCGTATTGTAGCG
*rob*Up-1	AACTAAGCTTTGCCATCGTACTACTAG
*rob*Up-2	GAGCAAAGACGCATCACAGCGGTCTGCTAAAATGAAATTC
*rob*Up-3	GAATTTCATTTTAGCAGACCGCTGTGATGCGTCTTTGCTC
*rob*Up-4	CGGCAAGCTTAATGAGGATATCAAGACG
*rob*Down-1	AACTAAGCTTATCACTCAGATCACCTTC
*rob*Down-2	GCGGAATCAGGGAGTGGTTCGTGCGCTATTTCTTCAATTC
*rob*Down-3	GAATTGAAGAAATAGCGCACGAACCACTCCCTGATTCCGC
*rob*Down-4	GTAAACAAAAATAAGCTTGGTCAGCC
SAOUHSC_2898-1	AACTAAGCTTATCACTCAGATCACCTTC
SAOUHSC_2898-2	GGCTTGATTCCTTCAGAAACGTGCGCTATTTCTTCAATTC
SAOUHSC_2898-3	GAATTGAAGAAATAGCGCACGTTTCTGAAGGAATCAAGCC

SAOUHSC_2898-4	GCGAATAAAGCTTCATCCATACG
SAOUHSC_2899-1	GCCGTCTTGGGATCCTCATTAAC
SAOUHSC_2899-2	GGATAATCAGCAGCATAAAGCGGTACACCTTTAGGATCTG
SAOUHSC_2899-3	CAGATCCTAAAGGTGTACCGCTTTATGCTGCTGATTATCC
SAOUHSC_2899-4	CTATGGATCCTTCTTCAGTATC
SAOUHSC_2900-1	TTAGGATCCAAAGGTGCGCTCATTATG
SAOUHSC_2900-2	GAATATAACCTAAGTGACCGCCAGGAATAAAGATGAGCAC
SAOUHSC_2900-3	GTGCTCATCTTTATTCCTGGCGGTCACTTAGGTTATATTC
SAOUHSC_2900-4	CTATTTTGGATCCGTTTACAAC
icaR-1	TGGTGAAGCTTGATCAACGATAGTATC
icaR-4	TAATAAAGCTTGATACCATCGTACTC
ica-1	AATTGGATCCTCATTGAACAAGAAGCC
ica-2	TAATACTAGTTGTCCCCCTTGAGCCCATC
ica-3	GATGAAACTAGTTATGAAAATGCTTATCC
ica-4	AATTGTAACACTAAGGATCCACCCTCC

qPCR

gyrB for	AGGTCTTGGAGAAATGAATG
gyrB rev	CAAATGTTTGGTCCGCTT
icaR for	CGCCTGAGGAATTTTCTG
icaR rev	GGATGCTTTCAAATACCAAC
icaA for	AGTTGTCGACGTTGGCTAC
icaA rev	CCAAAGACCTCCCAATGT
icaD for	ACCCAACGCTAAAATCATCG
icaD rev	GCGAAAATGCCCATAGTTTC
icaB for	ATACCGGCAACTGGGTTTAT
icaB rev	TGCAAATCGTGGGTATGTGT
icaC for	CTTGGGTATTTGCACGCATT
icaC rev	GCAATATCATGCCGACACCT
SAOUHSC_2898 for	ATTGACACCTCGTGACGTTG
SAOUHSC_2898 rev	CCACTTGATACGTTGACGAC

EMSA and DNase I footprint analysis

ica-p-F	ATTGCGTTATCAATAATCTTATCCTTC
ica-p-R (5-Biotin)	TTGCAATTCCTTTACCTACCTTTC
ica-p-R’	TTGCAATTCCTTTACCTACCTTTC
ica-p-F-s1	ACAAATATTTCCGTTTAATTATAACAAC

ica-p-F-s2	AATCTATTGCAAATTAAAATACTATC
5bp-deletion-2	TTGTTGTTATAATTAAACGGTTTGTAATTGCAACTTAATT
5bp-deletion-3	AATTAAGTTGCAATTACAAACCGTTTAATTATAACAACAA
rob-p-F	CGTCTTTGCTCTCTAGTTAAAGAC
rob-p-R	CTATTCTCTTTTGCATCTTTTCGC
T7 promoter-1 cy3[a]	TAATACGACTCACTATAGGG
Fp-M13-F	GTTTTCCCAGTCACGAC
Fp-M13-R 6-FAM[b]	CAGGAAACAGCTATGAC
pET-28a-Rob-F	AGGTGGATCCATGCGAAAAGATGC
pET-28a-Rob-R	TAACAAGCTTTTAGTCATTACGTCCCACC
pET-22b-IcaR-F	GGAATTCCATATGCACCACCACCACCACCACTTGAAGGAT AAGATTATTGATAACGC
pET-22b-IcaR-R	CCCAAGCTTTTATTTCTTCAAAAATATATTTAGTAGCG

[a] cy3 labeled at the 5' end.

[b] 6-FAM labeled at the 5' end.

TABLE S1 List of genes up-regulated in microarray experiments

MW2 (TF2758) open reading frame	Name	Product	Fold[a]		
MW2495 (*satf2580*)		Glyoxalase protein	40.83	16.41	25.94
MW2496 (*satf2581*)		NmrA-like family protein	36.14	34.99	40.18
MW2497 (*satf2582*)		Conserved hypothetical protein	34.04	18.41	28.12
MW2498 (*satf2583*)	*rob*	Transcriptional regulator	47.86	29.38	20.46
MW2499 (*satf2584*)		2-deoxy-D-gluconate 3-dehydrogenase	41.21	32.51	24.43
MW2500(*satf2585*)		Amidohydrolase family protein	22.13	34.51	18.32
MW2501 (*satf2586*)		Putative hydrolase	10.89	5.27	4.29
MW2586 (*satf2686*)	*icaA*	intercellular adhesion protein A	6.01	2.76	1.75
MW2587 (*satf2687*)	*icaD*	intercellular adhesion protein D	5.59	3.72	5.36
MW2588 (*satf2688*)	*icaB*	intercellular adhesion protein B	8.05	6.35	6.25
MW2589 (*satf2689*)	*icaC*	intercellular adhesion protein C	7.82	1.92	6.12

[a] Fold changes indicate increases in expression levels in TF2758 from ATCC49775. Experiments were repeated three times.

Figure 1

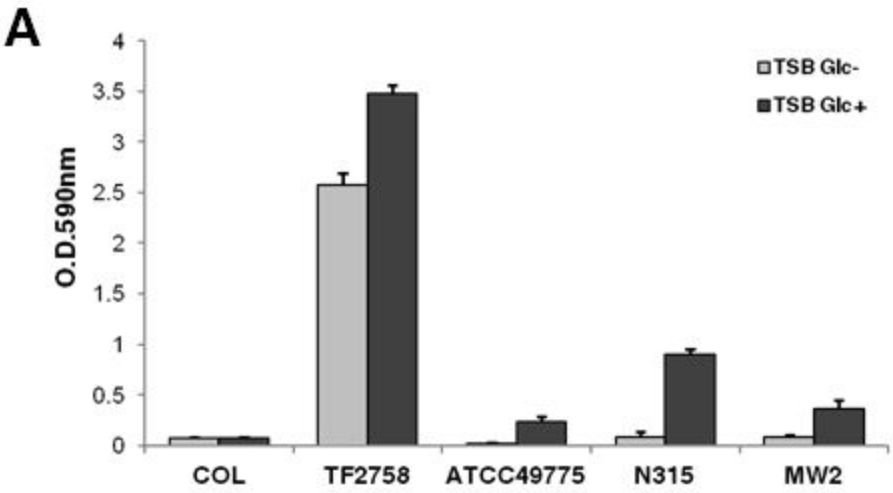
A
O.D.590nm
4
3.5
3
2.5
2
1.5
1
0.5
0
TSB Glc-
TSB Glc+
COL
TF2758
ATCC49775
N315
MW2

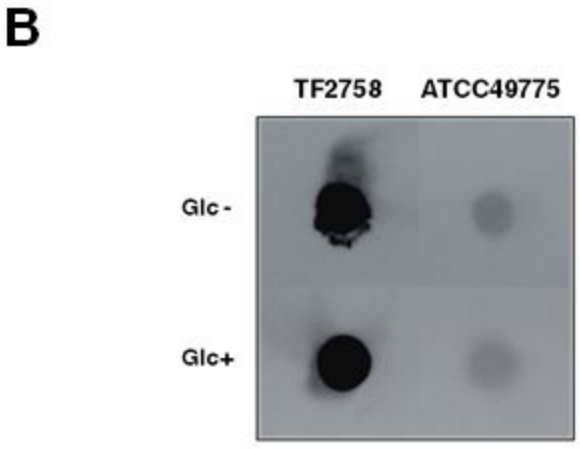
B
TF2758
ATCC49775
Glc -
Glc+

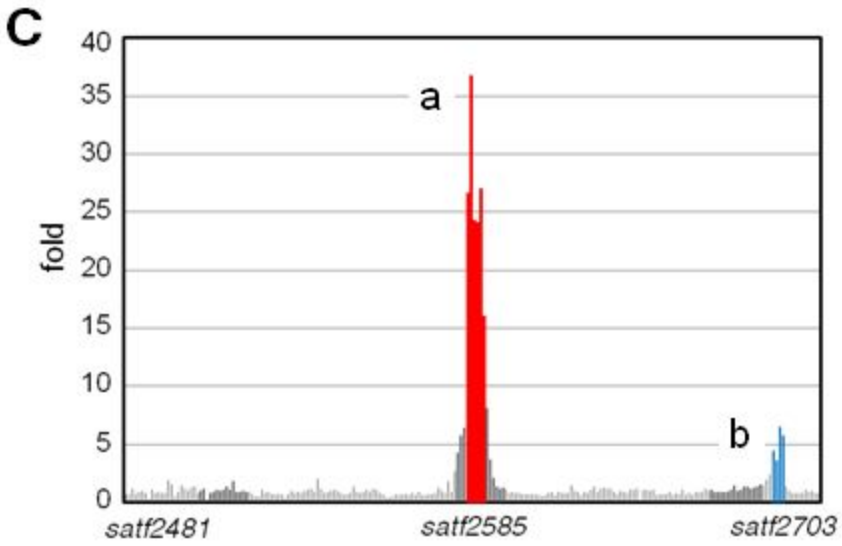
C
fold
40
35
30
25
20
15
10
5
0
a
b
satf2481
satf2585
satf2703

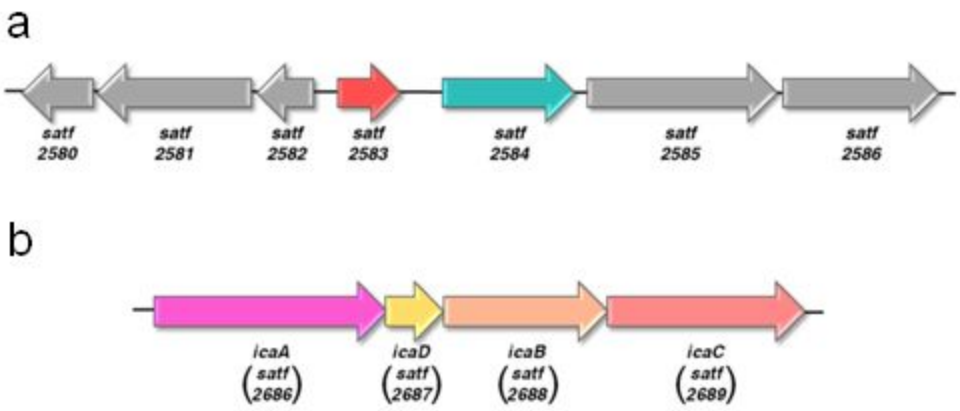
a
satf 2580
satf 2581
satf 2582
satf 2583
satf 2584
satf 2585
satf 2586
b
icaA (satf 2686)
icaD (satf 2687)
icaB (satf 2688)
icaC (satf 2689)

Figure 2

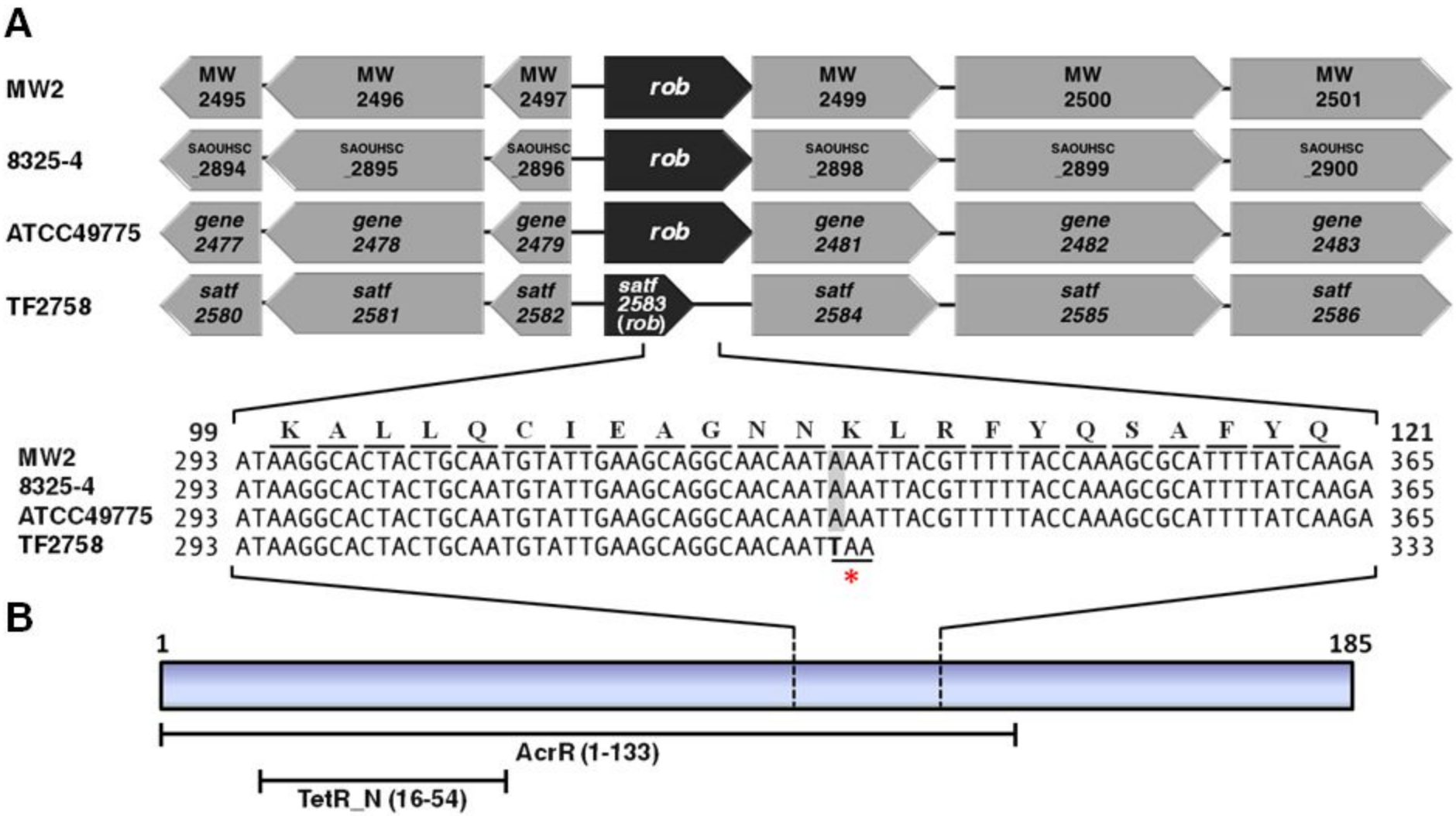
A
MW2
MW 2495
MW 2496
MW 2497
rob
MW 2499
MW 2500
MW 2501
8325-4
SAOUHSC _2894
SAOUHSC _2895
SAOUHSC _2896
rob
SAOUHSC _2898
SAOUHSC _2899
SAOUHSC _2900
ATCC49775
gene 2477
gene 2478
gene 2479
rob
gene 2481
gene 2482
gene 2483
TF2758
satf 2580
satf 2581
satf 2582
satf 2583 (rob)
satf 2584
satf 2585
satf 2586
99 K A L L Q C I E A G N N K L R F Y Q S A F Y Q 121
MW2 293 ATAAGGCACTACTGCAATGTATTGAAGCAGGCAACAATAAATTACGTTTTTACCAAAGCGCATTTTATCAAGA 365
8325-4 293 ATAAGGCACTACTGCAATGTATTGAAGCAGGCAACAATAAATTACGTTTTTACCAAAGCGCATTTTATCAAGA 365
ATCC49775 293 ATAAGGCACTACTGCAATGTATTGAAGCAGGCAACAATAAATTACGTTTTTACCAAAGCGCATTTTATCAAGA 365
TF2758 293 ATAAGGCACTACTGCAATGTATTGAAGCAGGCAACAATTAA 333
*
B
1
185
AcrR (1-133)
TetR_N (16-54)

Figure 3

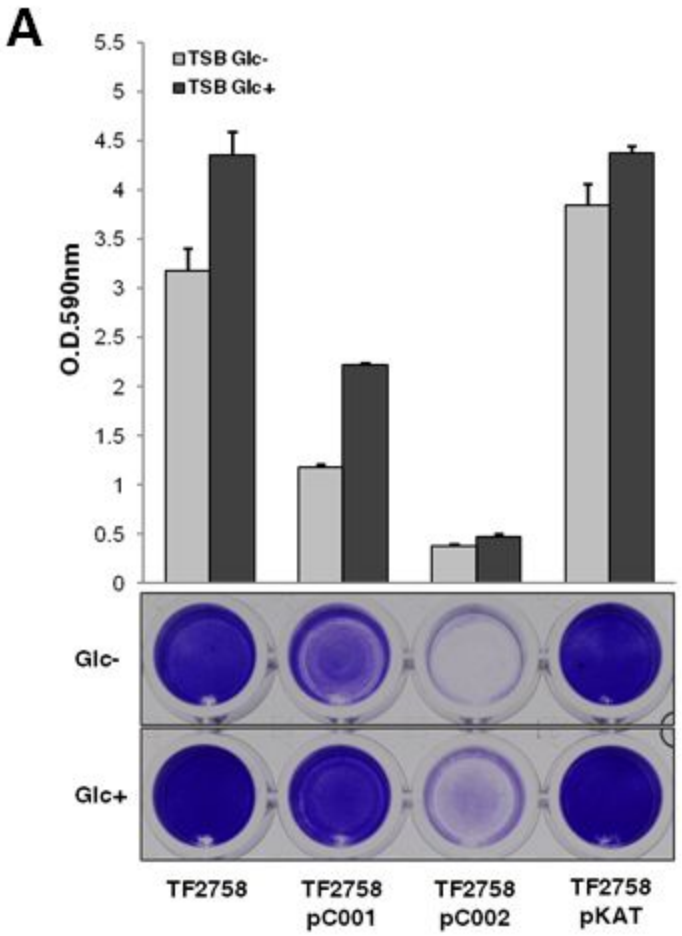
A
TSB Glc-
TSB Glc+
O.D.590nm
5.5
5
4.5
4
3.5
3
2.5
2
1.5
1
0.5
0
Glc-
Glc+
TF2758
TF2758 pC001
TF2758 pC002
TF2758 pKAT

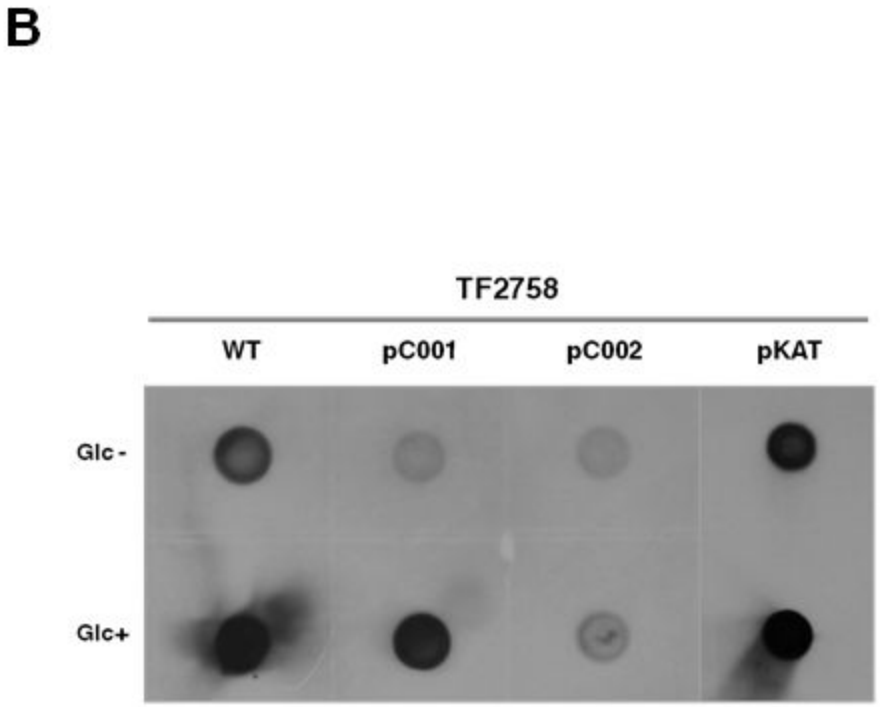
B
TF2758
WT
pC001
pC002
pKAT
Glc -
Glc+

Figure 4

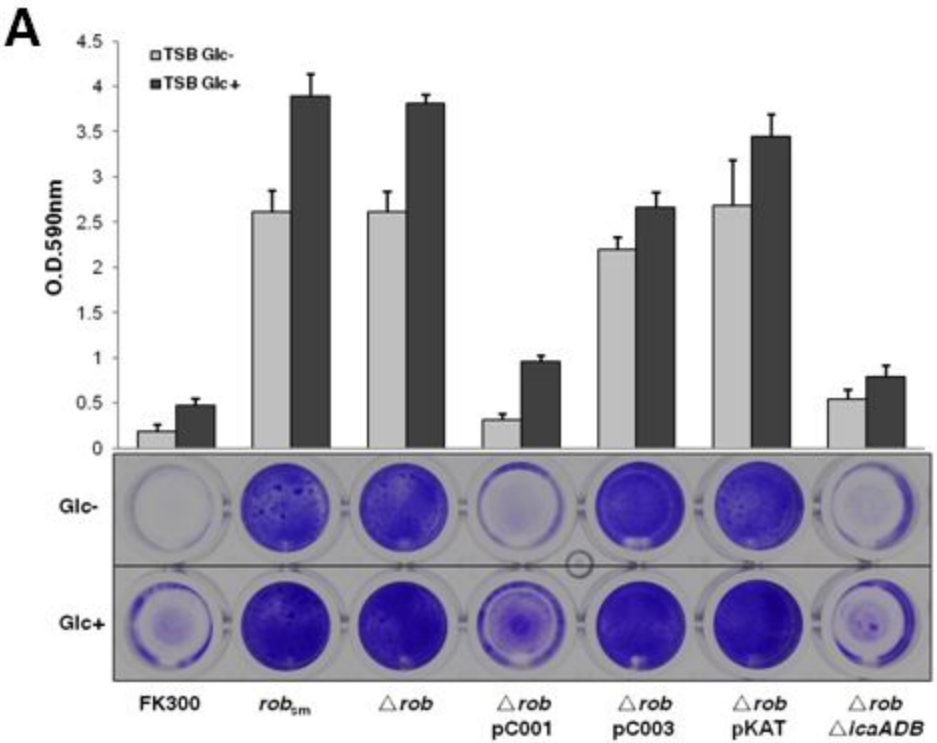
A
TSB Glc-
TSB Glc+
O.D.590nm
4.5
4
3.5
3
2.5
2
1.5
1
0.5
0
Glc-
Glc+
FK300
robsm
△rob
△rob pC001
△rob pC003
△rob pKAT
△rob △icaADB

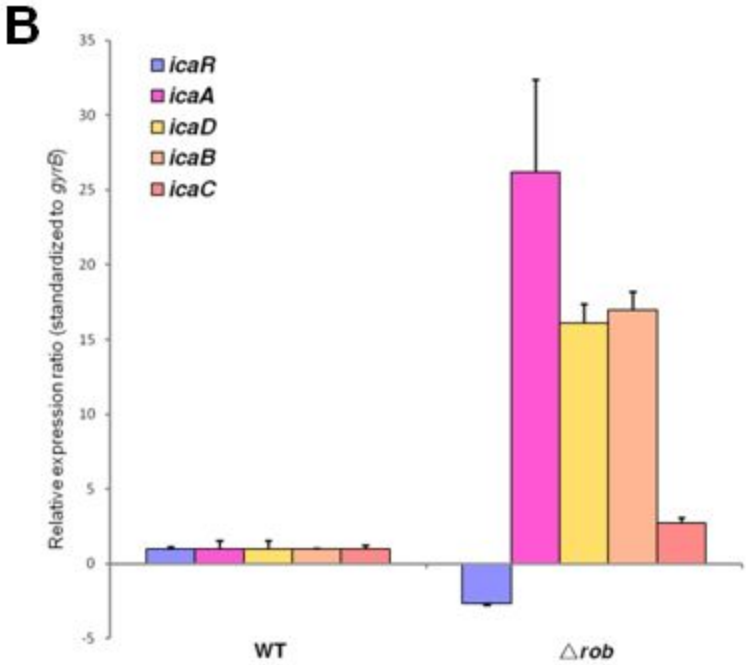
B
icaR
icaA
icaD
icaB
icaC
Relative expression ratio (standardized to gyrB)
35
30
25
20
15
10
5
0
-5
WT
△rob

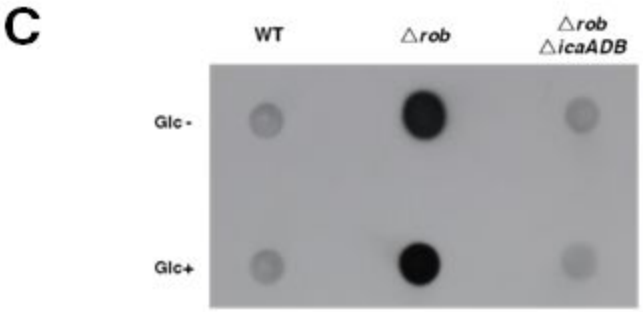
C
WT
△rob
△rob △icaADB
Glc-
Glc+

Figure 5

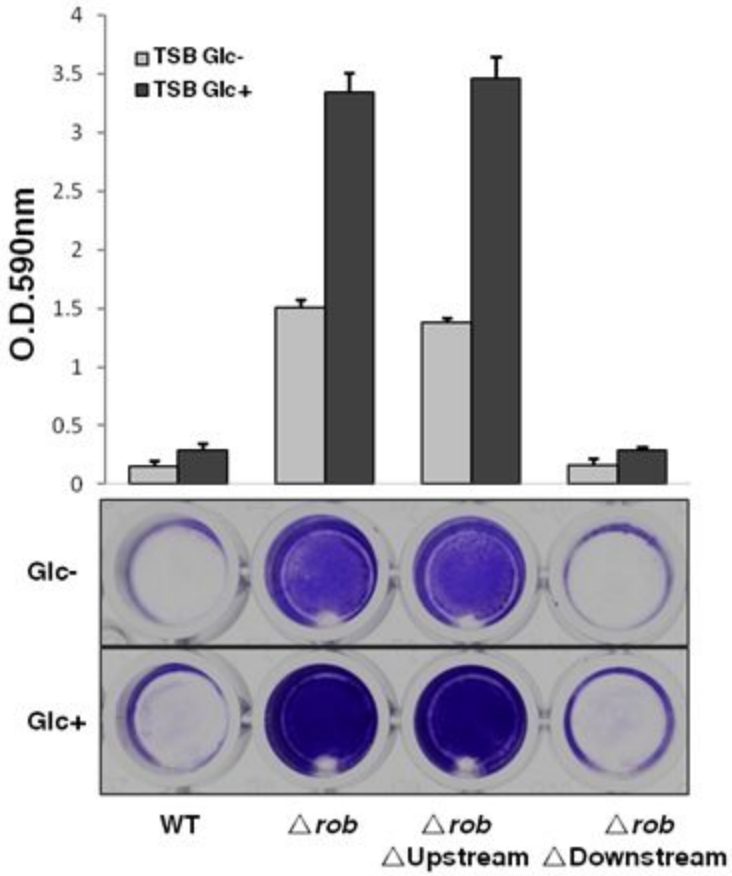
O.D.590nm
4
3.5
3
2.5
2
1.5
1
0.5
0
TSB Glc-
TSB Glc+
Glc-
Glc+
WT
△rob
△rob △Upstream
△rob △Downstream

Figure 6

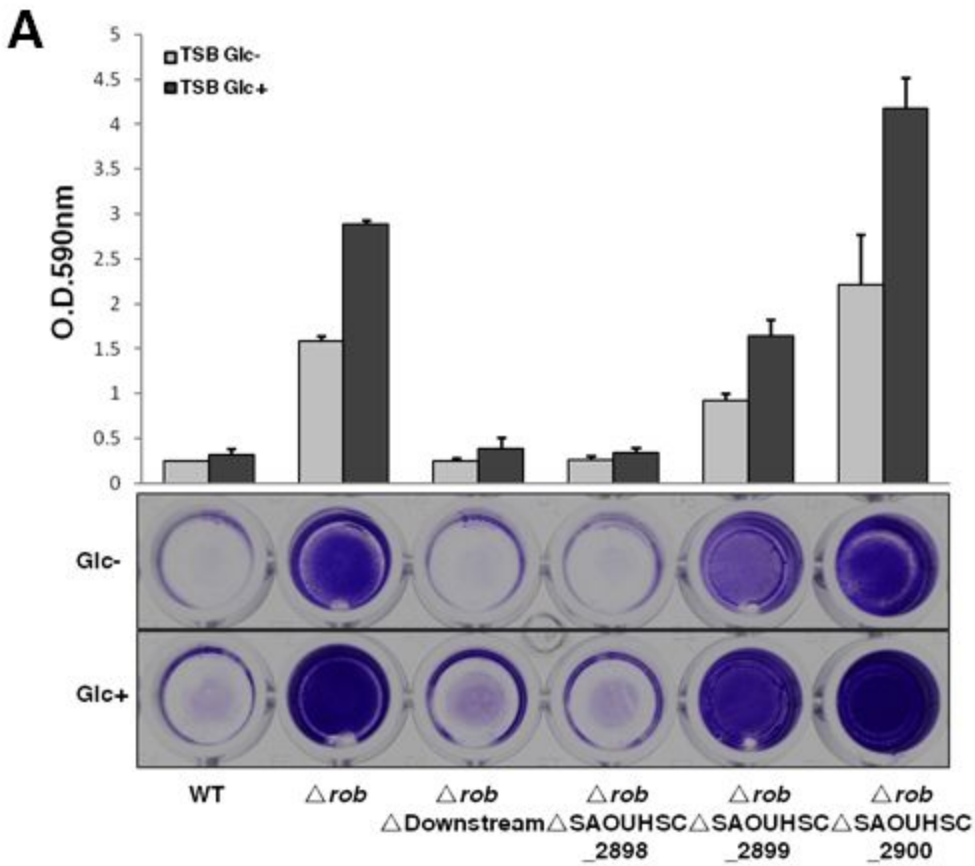
A
TSB Glc-
TSB Glc+
O.D.590nm
5
4.5
4
3.5
3
2.5
2
1.5
1
0.5
0
Glc-
Glc+
WT
△rob
△rob △Downstream
△rob △SAOUHSC_2898
△rob △SAOUHSC_2899
△rob △SAOUHSC_2900

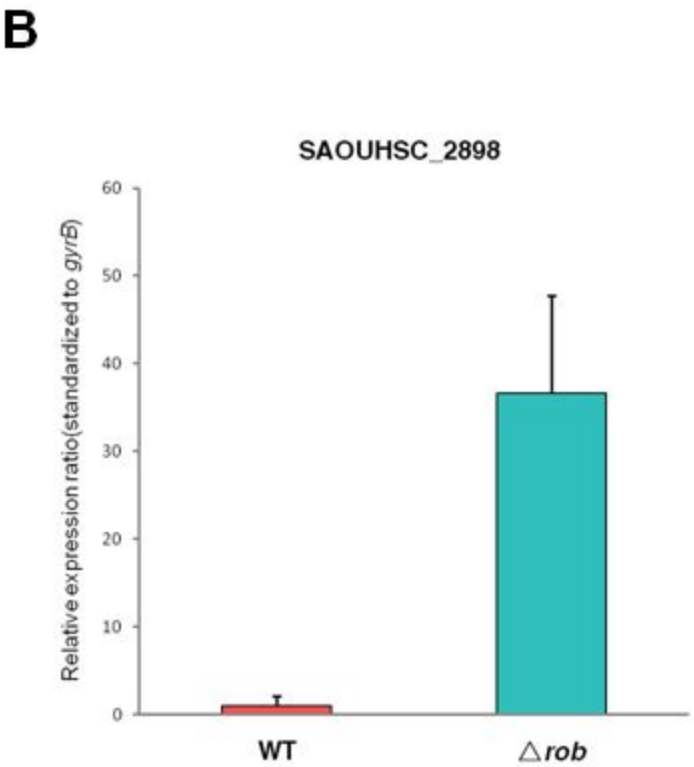
B
SAOUHSC_2898
Relative expression ratio(standardized to gyrB)
60
50
40
30
20
10
0
WT
△rob

Figure 7

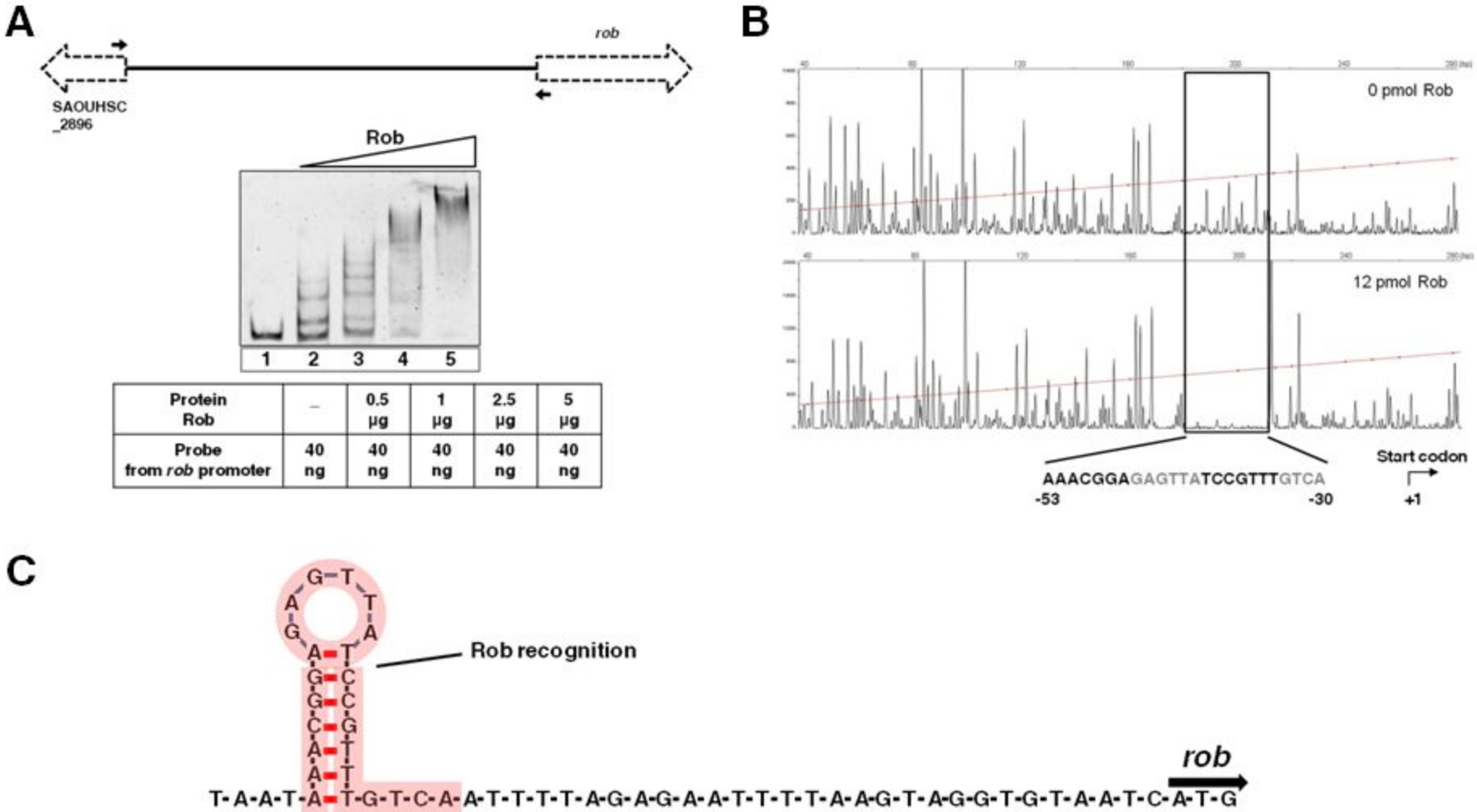
A
rob
SAOUHSC
_2896
Rob
1 2 3 4 5
Protein Rob | – | 0.5 µg | 1 µg | 2.5 µg | 5 µg
Probe from rob promoter | 40 ng | 40 ng | 40 ng | 40 ng | 40 ng
B
0 pmol Rob
12 pmol Rob
AAACGGAGAGTTATCCGTTTGTCA
-53
-30
Start codon
+1
C
Rob recognition
rob
T-A-A-T-A-T-G-T-C-A-A-T-T-T-T-A-G-A-G-A-A-T-T-T-T-A-A-G-T-A-G-G-T-G-T-A-A-T-C-A-T-G

Figure 8

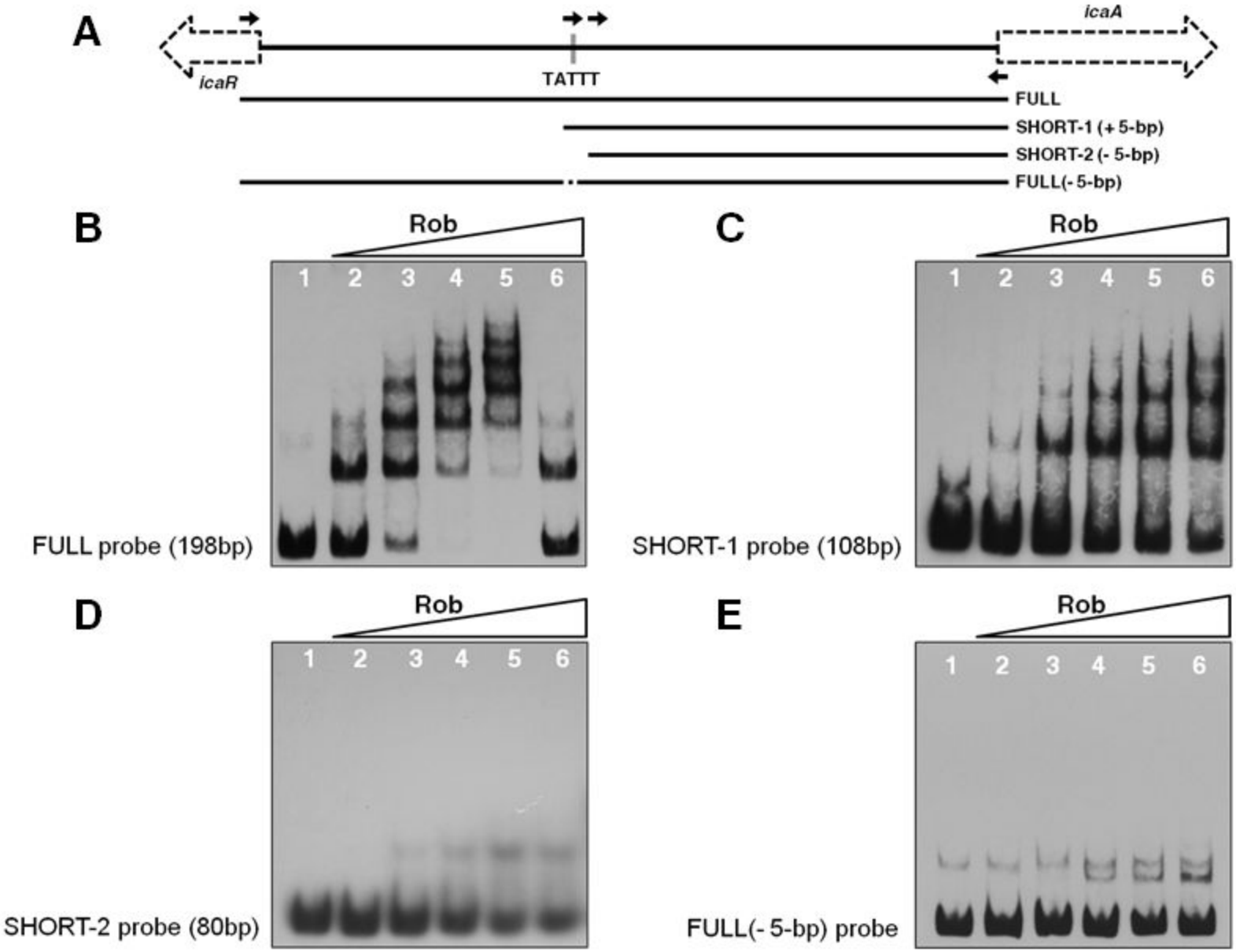
A
icaA
icaR
TATTT
FULL
SHORT-1 (+ 5-bp)
SHORT-2 (- 5-bp)
FULL(- 5-bp)
B
Rob
1 2 3 4 5 6
FULL probe (198bp)
C
Rob
1 2 3 4 5 6
SHORT-1 probe (108bp)
D
Rob
1 2 3 4 5 6
SHORT-2 probe (80bp)
E
Rob
1 2 3 4 5 6
FULL(- 5-bp) probe

Figure 9

A

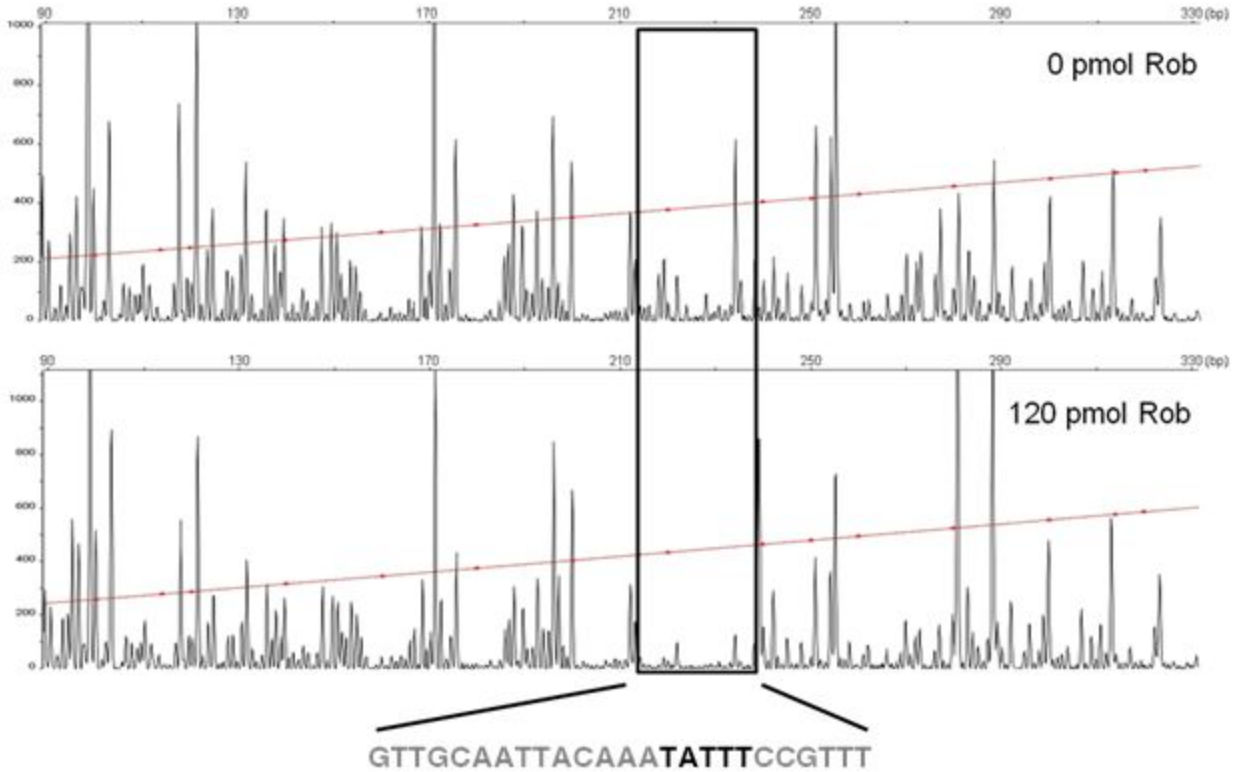

B

```
Binding site of Rob to rob promoter   1        AAACGGAGAGTTATCCGTTTGTCA  24
Binding site of Rob to ica promoter   1  GTTGCAATTACAAATATTTCCGTTT        25
                                            **     * *   *  *******
```

Figure 10

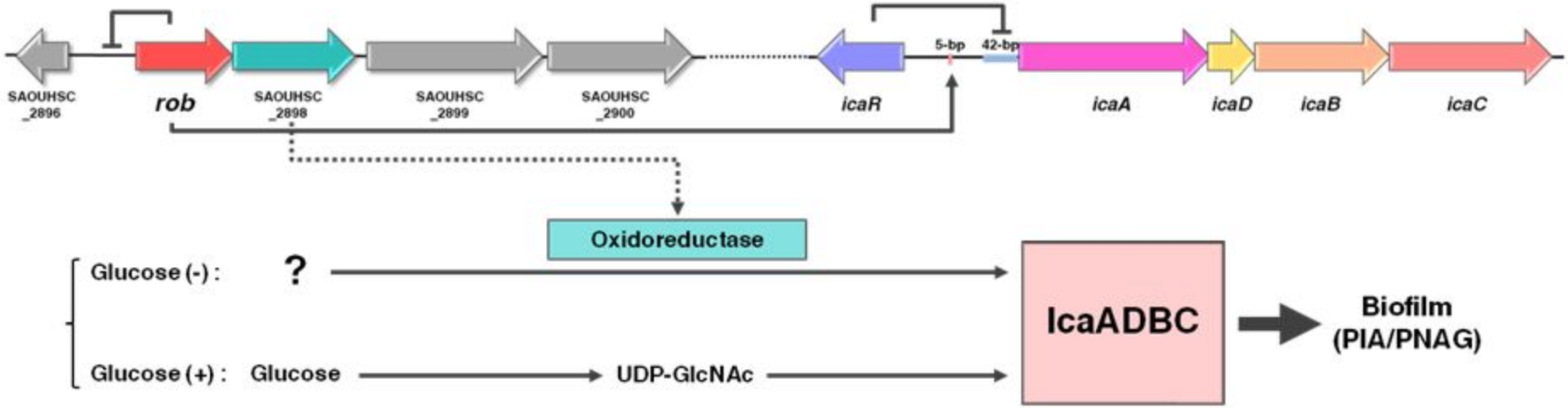
SAOUHSC _2896
rob
SAOUHSC _2898
SAOUHSC _2899
SAOUHSC _2900
icaR
5-bp
42-bp
icaA
icaD
icaB
icaC
Oxidoreductase
Glucose (-) :
?
Glucose (+) :
Glucose
UDP-GlcNAc
IcaADBC
Biofilm (PIA/PNAG)

Figure S1

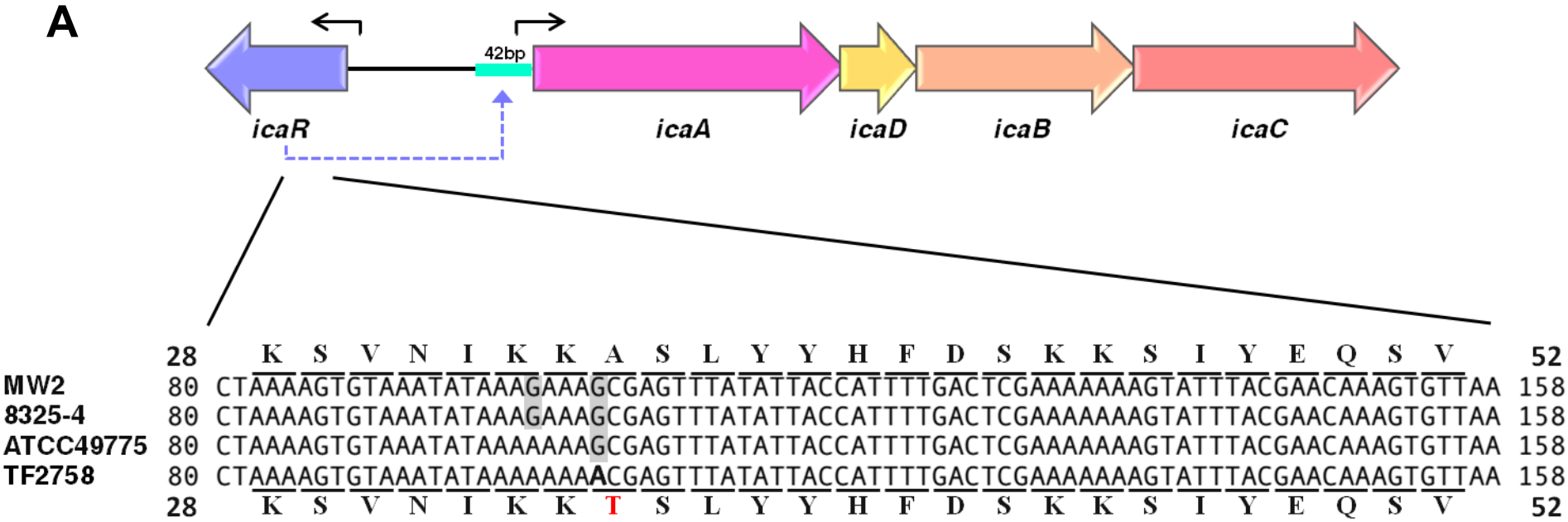
A
42bp
icaR
icaA
icaD
icaB
icaC
28 K S V N I K K A S L Y Y H F D S K K S I Y E Q S V 52
MW2 80 CTAAAAGTGTAAATATAAAGAAAGCGAGTTTATATTACCATTTTGACTCGAAAAAAAGTATTTACGAACAAAGTGTTAA 158
8325-4 80 CTAAAAGTGTAAATATAAAGAAAGCGAGTTTATATTACCATTTTGACTCGAAAAAAAGTATTTACGAACAAAGTGTTAA 158
ATCC49775 80 CTAAAAGTGTAAATATAAAAAAAGCGAGTTTATATTACCATTTTGACTCGAAAAAAAGTATTTACGAACAAAGTGTTAA 158
TF2758 80 CTAAAAGTGTAAATATAAAAAAAACGAGTTTATATTACCATTTTGACTCGAAAAAAAGTATTTACGAACAAAGTGTTAA 158
28 K S V N I K K T S L Y Y H F D S K K S I Y E Q S V 52

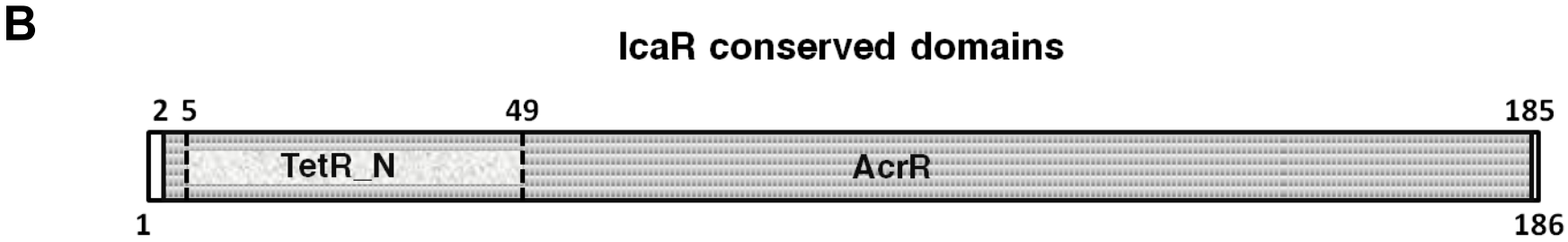
B
IcaR conserved domains
2 5
49
185
TetR_N
AcrR
1
186

Figure S2

A

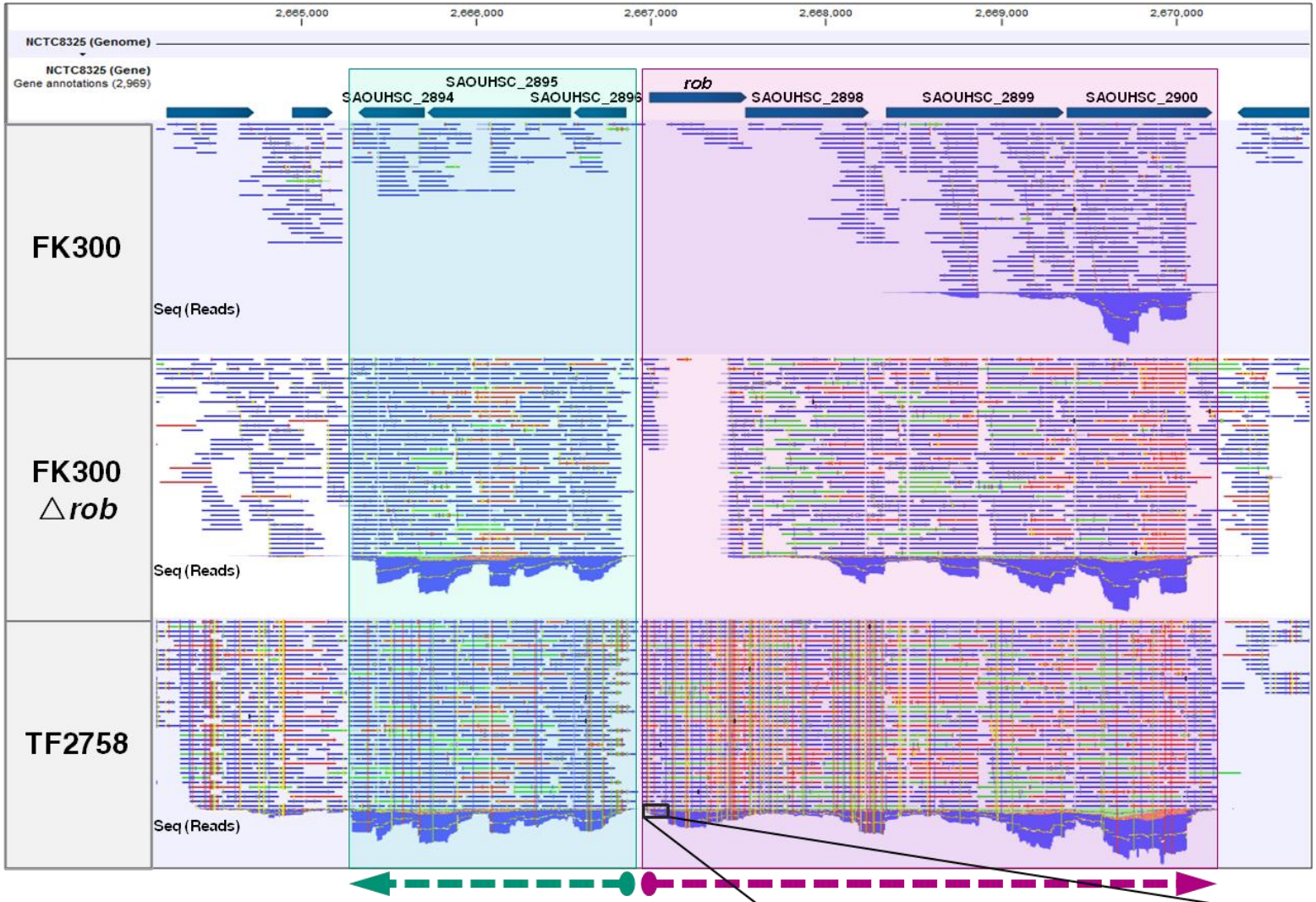
2,665,000
2,666,000
2,667,000
2,668,000
2,669,000
2,670,000
NCTC8325 (Genome)
NCTC8325 (Gene)
Gene annotations (2,969)
SAOUHSC_2895
SAOUHSC_2894
SAOUHSC_2896
rob
SAOUHSC_2898
SAOUHSC_2899
SAOUHSC_2900
FK300
Seq (Reads)
FK300
△rob
Seq (Reads)
TF2758
Seq (Reads)

B


Putative -35
CATTATCAACACTCTTTTCTTTTATGATATTTAATAGTTATTGCAAATTCATTGCTAACTTTCTTAAC
GTAATAGTTGTGAGAAAAGAAAATACTATAAATTATCAATAACGTTTAAGTAACGATTGAAAGAATTG
Putative -10
rob
ACGTTTTATAATAAACGGAGAGTTATCCGTTTGTCAATTTTAGAGAACTATAAGTAGGTGGAATCATG
TGCAAAATATTATTTGCCTCTCAATAGGCAAACAGTTAAAATCTCTTGATATTCATCCACCTTAGTAC
GAGAGTTATCCGTTTGTCAATTTTAGAGAACTATAAGTAGGTGGAATCATG
GAGAGTTATCCGTTTGTCAATTTTAGAGAACTATAAGTAGGTGGAATCATG
GAGAGTTATCCGTTTGTCAATTTTAGAGAACTATAAGTAGGTGGAATCATG
GAGAGTTATCCGTTTGTCAATTTTAGAGAACTATAAGTAGGTGGAATCATG
GAGAGTTATCCGTTTGTCAATTTTAGAGAACTATAAGTAGGTGGAATCATG
GAGAGTTATCCGTTTGTCAATTTTAGAGAACTATAAGTAGGTGGAATCATG

Figure S3

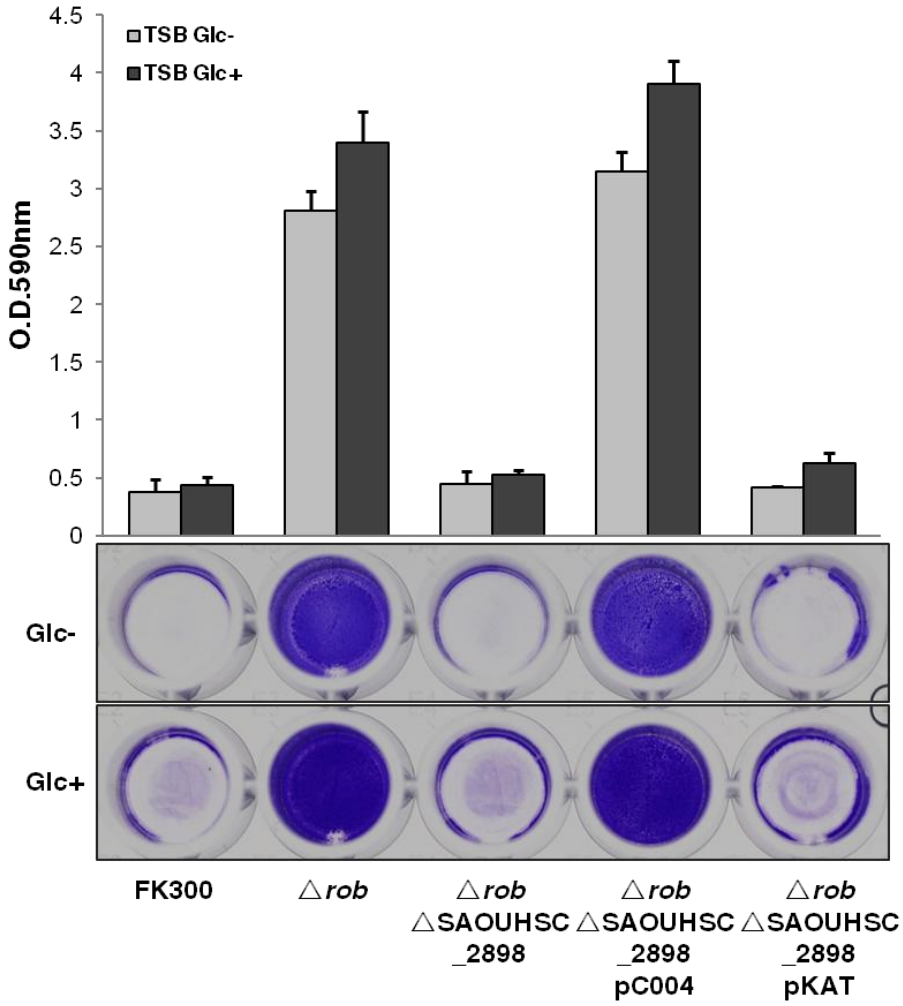
TSB Glc-
TSB Glc+
O.D.590nm
4.5
4
3.5
3
2.5
2
1.5
1
0.5
0
Glc-
Glc+
FK300
△rob
△rob △SAOUHSC _2898
△rob △SAOUHSC _2898 pC004
△rob △SAOUHSC _2898 pKAT

Figure S4

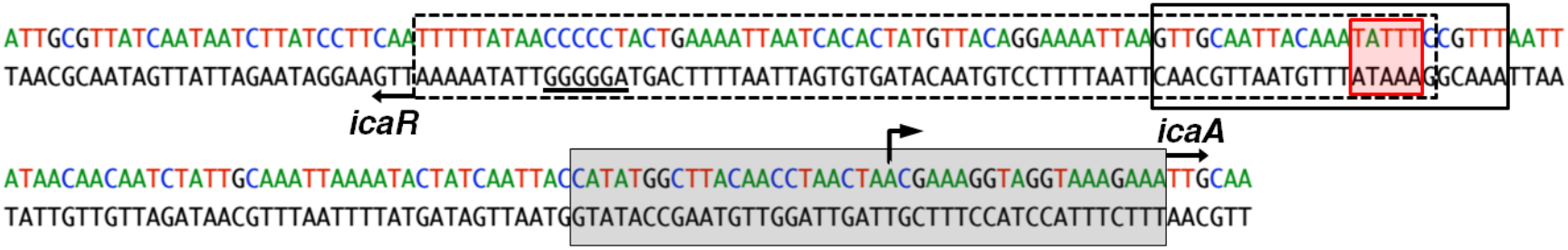
ATTGCGTTATCAATAATCTTATCCTTCAATTTTTATAACCCCCTACTGAAAATTAATCACACTATGTTACAGGAAAATTAAGTTGCAATTACAAATATTTGCGTTTAATT
TAACGCAATAGTTATTAGAATAGGAAGTTAAAAATATTGGGGGATGACTTTTAATTAGTGTGATACAATGTCCTTTTAATTCAACGTTAATGTTTATAAAGGCAAATTAA
icaR
icaA
ATAACAACAATCTATTGCAAATTAAAATACTATCAATTACCATATGGCTTACAACCTAACTAACGAAAGGTAGGTAAAGAAATTGCAA
TATTGTTGTTAGATAACGTTTAATTTTATGATAGTTAATGGTATACCGAATGTTGGATTGATTGCTTTCCATCCATTTCTTTAACGTT

Figure S5

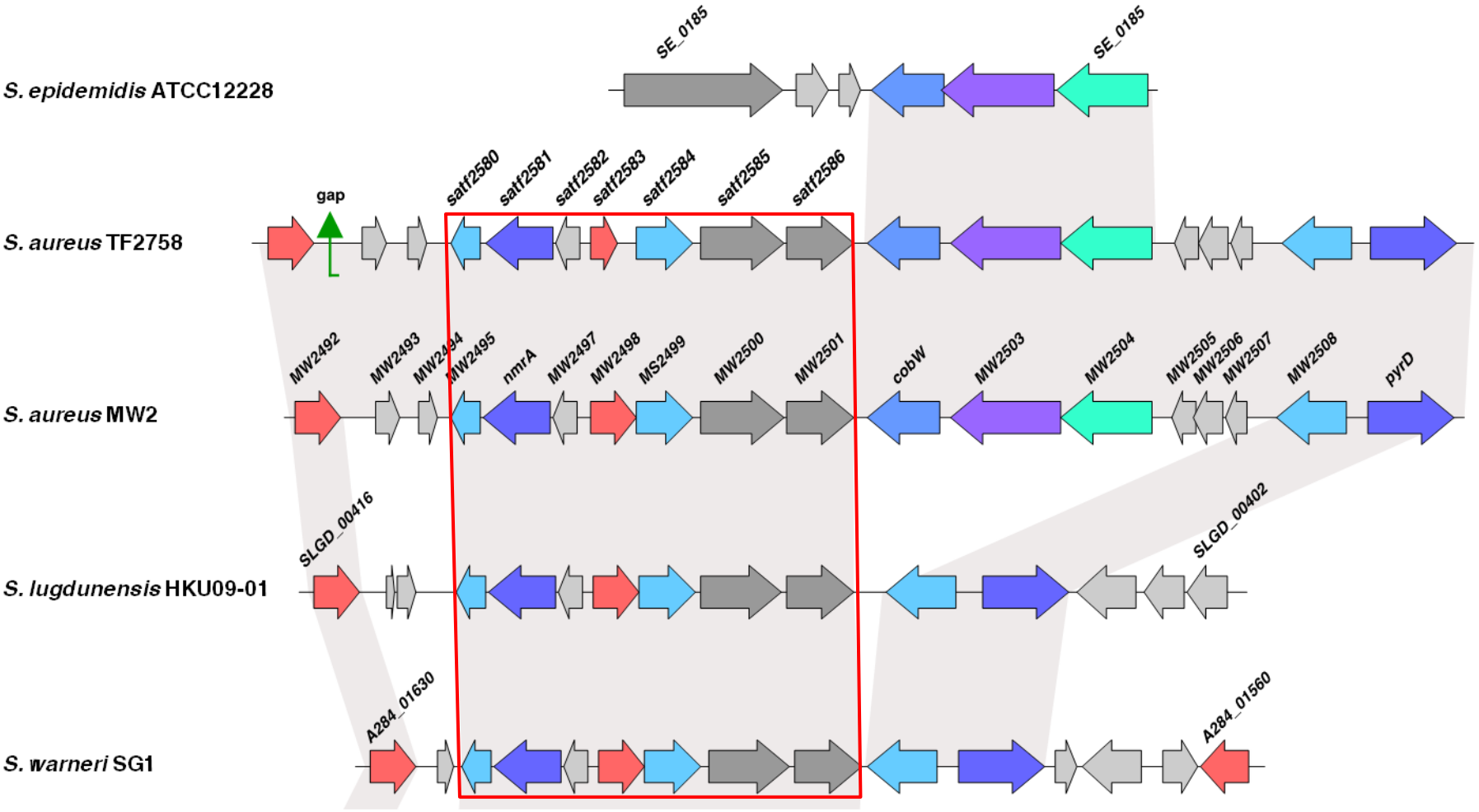
S. epidemidis ATCC12228
SE_0185
SE_0185
S. aureus TF2758
gap
satf2580
satf2581
satf2582
satf2583
satf2584
satf2585
satf2586
S. aureus MW2
MW2492
MW2493
MW2494
MW2495
nmrA
MW2497
MW2498
MS2499
MW2500
MW2501
cobW
MW2503
MW2504
MW2505
MW2506
MW2507
MW2508
pyrD
S. lugdunensis HKU09-01
SLGD_00416
SLGD_00402
S. warneri SG1
A284_01630
A284_01560